UltraRapid Communication

Identification of Pathways for Atherosclerosis in Mice

Integration of Quantitative Trait Locus Analysis and Global Gene Expression Data

Susanna S. Wang, Eric E. Schadt, Hui Wang, Xuping Wang, Leslie Ingram-Drake, Weibin Shi, Thomas A. Drake, Aldons J. Lusis

Abstract—We report a combined genetic and genomic analysis of atherosclerosis in a cross between the strains C3H/HeJ and C57BL/6J on a hyperlipidemic apolipoprotein E–null background. We incorporated sex and sex-by-genotype interactions into our model selection procedure to identify 10 quantitative trait loci for lesion size, revealing a level of complexity greater than previously thought. Of the known risk factors for atherosclerosis, plasma triglyceride levels and plasma glucose to insulin ratios were particularly strongly, but negatively, associated with lesion size. We performed expression array analysis for 23 574 transcripts of the livers and adipose tissues of all 334 F2 mice and identified more than 10 000 expression quantitative trait loci that either mapped to the gene encoding the transcript, implying *cis* regulation, or to a separate locus, implying *trans*-regulation. The gene expression data allowed us to identify candidate genes that mapped to the atherosclerosis quantitative trait loci and for which the expression was regulated in *cis*. Genes highly correlated with lesions were enriched in certain known pathways involved in lesion development, including cholesterol metabolism, mitochondrial oxidative phosphorylation, and inflammation. Thus, global gene expression in peripheral tissues can reflect the systemic perturbations that contribute to atherosclerosis. **(*Circ Res*. 2007;101:e11-e30.)**

Key Words: atherosclerosis ■ quantitative trait locus ■ C3H/HeJ ■ expression arrays ■ sex

Atherosclerosis, the primary cause of coronary artery disease (CAD), is a complex trait resulting from the interaction of a large number of genetic and environmental factors. Candidate gene studies in human populations have been only modestly successful in identifying genes involved in the disease, and the complexity and heterogeneity of the disease have made genome-wide approaches difficult.[1] One approach for the dissection of this complex trait has been to study genetic models in rodents. More than 100 knockout mouse models have effects on the disease, but these extreme variations do not reflect the more subtle gene–gene and gene–environment interactions that underlie the common forms of CAD.[2] Quantitative trait locus (QTL) analyses of crosses between inbred strains of mice differing in atherosclerosis susceptibility have convincingly mapped loci that segregate with lesion development, but the underlying genes have been difficult to identify, because the linked regions usually harbor hundreds of genes.[3]

We and others have recently shown that gene transcript levels can provide useful intermediate phenotypes between DNA variation and complex clinically relevant traits such as adiposity in genetic crosses in mice.[4–7] Thus, when the transcript levels of genes are quantified using whole-genome expression arrays in segregating populations of mice, the loci determining the levels can be mapped by QTL analysis. The loci, termed expression QTLs or expression QTLs (eQTLs), are considered to be *cis*-acting if the locus controlling a given transcript maps to the gene encoding that transcript or *trans*-acting if the locus maps elsewhere. In a cross consisting of 111 female F2 mice derived from the parental strains DBA/2J and C57BL/6J, we identified more than 4000 eQTLs with logarithm of the odds (LOD) scores exceeding 4.3,[4] and in a subsequent study, we validated the eQTLs using a classic *cis*/*trans* test.[8] The *cis*-acting eQTLs that colocalize with a clinical trait QTLs (cQTLs) are proving very useful in prioritizing positional candidate genes.[9–12] More importantly, genes that are likely to be involved in pathways contributing to a clinical trait can be identified by testing for correlations between transcript levels and the clinical trait and then assessing whether these correlated pairs support a causal, reactive or independent relationship with respect to one or more QTLs.[13]

We report here a large genetic cross in which we have quantified atherosclerotic lesions as well as whole-genome transcript levels, making possible the above approaches. The cross was constructed using 2 strains of mice that differ dramatically in lesion susceptibility: C3H/HeJ (resistant) and C57BL/6J (susceptible). To examine genetic factors contributing to advanced lesions, the cross was performed on the background

Original received October 26, 2006; resubmission received March 28, 2007; revised resubmission received July 5, 2007; accepted July 6, 2007.

From the Departments of Human Genetics (S.S.W., L.I.-D., A.J.L.), Statistics (H.W.), Medicine (X.W., W.S., A.J.L.), and Pathology and Laboratory Medicine (L.I.-D., T.A.D.), University of California at Los Angeles; and Rosetta Inpharmatics LLC/Merck (E.E.S.), Seattle, Wash. Present address for W.S.: Department of Radiology, University of Virginia, Charlottesville.

Correspondence to Aldons J. Lusis, Department of Medicine, 675 Charles E Young Dr South, 3730 MRL, University of California, Los Angeles, CA 90095-1679. E-mail jlusis@mednet.ucla.edu

Circulation Research **is available at http://circres.ahajournals.org** **DOI: 10.1161/CIRCRESAHA.107.152975**

of an apolipoprotein E (*ApoE*)-null mutation, and mice were then fed a high-fat "western" diet.[14] Our results reveal a highly complex genetic structure for atherosclerosis susceptibility, with 10 loci contributing to lesion development. This contrasts with previous studies that suggested only 1 or 2 significant loci.[15,16] The individual loci exhibit striking sex dependence, as most of the loci are sex-biased and some are essentially sex specific. Liver and adipose tissue global gene expression analyses revealed candidate genes and identified pathways associated with atherosclerosis.

Materials and Methods

Mice and Diets

C57BL/6J *ApoE*$^{-/-}$ (B6 *ApoE*$^{-/-}$) mice were purchased from the The Jackson Laboratory (Bar Harbor, Me) and C3H/HeJ *ApoE*$^{-/-}$ (C3H *ApoE*$^{-/-}$) mice were bred by backcrossing B6 *ApoE*$^{-/-}$ to C3H/HeJ for 10 generations.[17] All mice were fed ad libitum and maintained on a 12-hour light/dark cycle. F2 mice were generated by crossing B6 *ApoE*$^{-/-}$ with C3H *ApoE*$^{-/-}$ and subsequently intercrossing the F1s. Approximately 80% of the parental breeding pairs consisted of B6 females and C3H males, and 20% of the breeding pairs consisted of the reciprocal cross. The mice were fed Purina Chow (Ralston-Purina Co, St Louis, Mo) containing 4% fat until 8 weeks of age and then transferred to a western diet (Teklad 88137, Harlan Teklad, Madison Wis) containing 42% fat and 0.15% cholesterol for 16 weeks until euthanasia at 24 weeks of age. Mice were fasted for 4 hours and anesthetized via exposure to isoflurane before blood was collected through the retroorbital sinus. Plasmas were stored at −80°C. We have performed other studies on this cross, namely a QTL and eQTL study for abdominal fat pad mass,[18] network analysis using weight,[19] and analysis of differential gene expression between the sexes across four tissues.[20] All procedures of housing and treatment of the animals were performed in accordance with IACUC regulations.

Histological Analyses, Lipid Measurements, and Quantification of Atherosclerosis Risk Factors

All 334 aortae were sectioned, and lesions were quantified.[21] After the mice were euthanized, the heart and proximal aorta were excised and washed in phosphate-buffered saline. The apex and lower half of the ventricles were removed. The remaining specimen was embedded in Tissue-Tek (Miles), frozen on dry ice, and stored at −80°C until sectioning. Serial cryosections were prepared through the ventricle until the aortic valves appeared. From then on, every fifth 10-μm section was collected on poly-D-lysine–coated slides until the aortic sinus was completely sectioned. Sections were stained with hematoxylin and oil red O, which specifically stains lipids. Slides were examined by light microscopy. The average fatty streak lesion area was quantified throughout the aortic sinus using an ocular with an micrometer-squared grid and was normalized to 40 sections. Plasma triglycerides, total cholesterol, unesterified cholesterol, high-density lipoprotein (HDL), low-density lipoprotein (LDL)/very-low-density lipoprotein (VLDL), glucose and free fatty acids, as well as hepatic triglycerides, total cholesterol, and unesterified cholesterol were assayed as previously described.[21] ELISA assays were used to measure plasma insulin (Alpco Diagnostics, Windham, NH), *Mcp-1* (R&D Systems, Minneapolis, Minn), leptin (Alpco Diagnostics), and adiponectin (Linco Research Inc, St Charles, Mo) levels.

Linkage and Data Analysis

A 1.5-cM-dense map was constructed using single-nucleotide polymorphism (SNP) markers using the multiple inversion probe technology (ParAllele Biosciences, Inc, San Francisco, Calif).[22] The SNP map was created according to Celera and National Center for Biotechnology Information public databases. Phenotypic traits were transformed as needed to normalize the residuals, which involved taking the natural log of some of the trait values. Outliers (>3 SD) were omitted. The high density of the SNP marker map allowed the use of single-marker linear regression to model QTL effects,[18] instead of inferring genotypes between markers through interval mapping. The general equation for linear regression was:

$$y_j=\beta_o+\beta_1x_{1j}+\beta_2x_{2j}+\varepsilon_j \quad (1)$$

where y_j is the trait value for the jth mouse, β_o is the trait mean, β_1x_{1j} represents the additive effect, β_2x_{2j} represents the dominant effect, and ε_j is the random error. To determine the genetic contribution to the trait, an F test was performed between the model and the null hypothesis:

$$y_j=\beta_o+\varepsilon_j \quad (2)$$

Because the distribution of atherosclerosis in males and females was significantly different and we wanted to maximize our power by using all animals, we analyzed all F2 animals together and accounted for sex by adding another variable, β_3x_{3j}, for sex, resulting in this equation:

$$y_j=\beta_o+\beta_1x_{1j}+\beta_2x_{2j}+\beta_3x_{3j}+\varepsilon_j \quad (3)$$

We were also interested in analyzing genotype–sex interactions. To model sex-additive (sex·add) and sex-dominant (sex·dom) interactive effects, we added 2 more variables, $\beta_4x_{1j}x_{3j}$ and $\beta_5x_{2j}x_{3j}$, respectively, to yield the following models:

$$y_j=\beta_o+\beta_1x_{1j}+\beta_2x_{2j}+\beta_3x_{3j}+\beta_4x_{1j}x_{3j}+\varepsilon_j \quad (4)$$

$$y_j=\beta_o+\beta_1x_{1j}+\beta_2x_{2j}+\beta_3x_{3j}+\beta_4x_{1j}x_{3j}+\beta_5x_{2j}x_{3j}+\varepsilon_j \quad (5)$$

For equations 3, 4 and 5, QTL analysis was performed using step-wise regression against the sex-only model:

$$y_j=\beta_o+\beta_3x_{3j}+\varepsilon_j \quad (6)$$

Not every locus exhibited significant sex·add or sex·dom interactions, and therefore inclusion of these terms at such loci decreased the power to detect QTLs.[18] To address this, we used a step-wise regression model, the model selection model, where the optimal model was chosen from among the 3 models represented above in equations 3, 4, and 5 for each SNP. The F statistic was used for this purpose. The step-wise procedure was performed as follows:

Step 1

The F test was performed between the model that included sex as a covariate (trait$\approx\mu$+add+dom+sex) and the null model (trait$\approx\mu$+sex).

Step 2

The significance of the additive term was assessed. If the additive term was not significant, we concluded there was no genetic contribution from this locus and the current model (trait$\approx\mu$+add+dom+sex) was the optimal model for this locus. The threshold for significance for this model was LOD>4.1.

Step 3

If the additive component was significant, the sex·add interaction term was considered, such that the model became trait$\approx\mu$+add+dom+sex+sex·add. The F test was performed between this model and the null model. If this model had a significantly improved fit over the previous model (trait$\approx\mu$+add+dom+sex) and had a lower Bayesian Information Criterion (BIC) than the previous model, then the sex·add term was incorporated into the model. The resulting LOD score had a genome-wide significance threshold of 4.7, where these thresholds are increased compared with those commonly applied[23] because of the increased degrees of freedom that result from incorporating sex and sex-by-QTL interactions into the genetic model. If the sex·add term failed to improve the fit of the model or exhibited a higher BIC than the previous model, then the sex·add term was excluded and the model without the sex-by-genotype interaction was the optimal model.

Step 4

If the sex·add term was significant, then the sex·dom term was considered, and thus the model became trait≈μ+add+dom+sex+sex·add+sex·dom. If the sex·dom term significantly improved the fit of the data and the BIC of this model (equation 5) was lower than that of the previous model (trait≈μ+add+dom+sex+sex·add), it was incorporated into the model and the significant threshold correspondingly increased to 5.3. Probability value thresholds corresponding to significant and suggestive LOD scores were 5×10^{-5} (genome-wide $P<0.05$) and 1×10^{-3}, respectively. If the sex·dom term failed to improve the fit of the model or if the model had an increased BIC compared with the previous model, the sex·dom term was dropped and the previous model (trait≈μ+add+dom+sex+sex·add) was the optimal model.

We performed 10 000 permutations on the data and computed genome-wide LOD scores for each permutation run and determined the LOD threshold, so that the fraction of eQTLs detected above that threshold in the permuted data were 0.05. To assess whether there were 2 peaks or 1 peak on chromosomes 1, 7, 9, and 11, for each pair of peak markers, we conditioned the trait value on one of the markers and computed the LOD score at the second marker using the residual values and vice versa. If the LOD score was significant under both conditions, then it likely is an independent peak.

QTL analysis was also performed for each sex separately using QTL Cartographer. Interval mapping was performed while considering additive and dominant effects.[24] These data were also permuted 10 000 times to establish a LOD score threshold of 4.2 for a genome-wide significance level of 0.05.

ANOVA between markers and traits was calculated using Statview v5.0 (SAS Institute Inc, Cary, NC). Correlations between lesions and lipids were calculated using the Spearman rank correlation. Data were then graphed in Sigma Plot (SPSS Inc, Chicago, Ill).

Global Gene Transcript Studies

RNA was isolated from the livers (n=311) and gonadal fat pads (n=305) of F2 mice using the TRIzol method and microarray analysis was performed.[4] Briefly, 60mer oligonucleotide chips were used (Agilent Technologies); all hybridizations were performed in duplicate with fluor reversal. Each individual sample was hybridized against the pool of F2 samples. Expression data can be obtained from Geo databases for liver (GSE2814) and adipose tissue (GSE3086). Significantly differentially expressed genes were determined as previously described.[25] Expression data in the form of mean log ratios (mlratios) were treated as a quantitative trait in eQTL analysis while taking genotype–sex interactions into account as described above.

eQTLs can be classified as *cis*- or *trans*-acting. The eQTLs that mapped to ±20 Mb of the gene encoding the transcript were assumed to correspond to *cis*-acting variations, although they could be explained by *trans*-acting effects (for example, by a nearby regulatory gene). The *cis*-eQTLs that colocalize with a lesion cQTLs within ±20 Mb were considered potential candidate genes for lesions. eQTLs that were not located within ±20 Mb of the gene were assumed to correspond to *trans*-acting variations in which the transcript abundance of a gene is controlled by a variation in a second, regulatory gene.

Gene Expression–Clinical Trait Correlation and Trait–Trait Correlations

Correlations between gene expression, measured as mlratios, and lesion area were calculated using step-wise linear regression with sex as an interactive covariate:

$$y_j=\beta_o+\beta_1x_{1j}+\beta_2x_{2j}+\beta_3x_{1j}x_{2j}+\varepsilon_j \quad (7)$$

where y_j is the trait value, β_o is the mean mlratio, β_1x_{1j} represents the mlratio effect, β_2x_{2j} represents the sex effect, and $\beta_3x_{1j}x_{2j}$ is the interaction between expression and sex components. The null hypothesis is the sex only model:

$$y_j=\beta_o+\beta_2x_{2j}+\varepsilon_j \quad (8)$$

An F test was performed between the full model and the sex-only model. Pearson correlation was also performed and adjusted for sex; both methods delivered similar results.

Correlations between traits were calculated using a partial Pearson correlation accounting for sex.

Pathway Analysis

Canonical pathways analysis is a method of identifying well-established and validated biochemical and functional pathways that are significantly enriched in a data set. We used Ingenuity Pathways Analysis to perform this function (IPA, Ingenuity Systems, Mountain View, CA). We analyzed 2 data sets: the first consisted of genes expressed in the liver that were correlated with atherosclerosis; the second consisted of genes expressed in adipose tissue that were correlated with atherosclerosis. We identified pathways curated by Ingenuity in the Ingenuity Pathways Knowledge Base that were overrepresented in these gene lists. The significance of the association between the data set and the canonical pathway was measured in 2 ways: (1) a ratio of the number of genes from the data set that map to the pathway divided by the total number of genes that map to the canonical pathway is displayed; (2) Fisher's exact test was used to calculate a probability value determining the probability that the enrichment between the genes in the dataset and the canonical pathway is explained by chance alone. The probability value is calculated using the right-tailed Fisher Exact Test.

Results

Genetic Determinants of Atherosclerosis for Advanced Lesions

C57BL/6J *ApoE*$^{-/-}$ mice are highly susceptible to atherosclerosis, whereas C3H/HeJ *ApoE*$^{-/-}$ mice are highly resistant.[17] To identify loci that contribute to this genetic difference in phenotype, a BXH *ApoE*$^{-/-}$ F2 population consisting of 334 mice (169 females, 165 males) was fed a western diet for 16 weeks to generate advanced atherosclerotic lesions. The mice were euthanized at 24 weeks of age and lesions from the aortic sinus were quantified. The distribution of lesion area ranged from 35 000 to 700 000 μm^2 per section. A dense genome scan (1.5-cM average spacing between markers) was performed using 1353 SNPs. Because of the high density of the markers genotyped in this cross, we used a single marker regression method to detect QTLs. To maximally power the detection of QTLs, we applied a regression model that included variables for additive and dominant genetic contributions, sex, and genotype-by-sex interactions: sex·add and sex·dom (see *Materials and Methods*).[18] We used a procedure similar to forward step-wise regression starting with this model: trait≈add+dom+sex (Equation 3) and including or excluding the 2 genotype–sex interaction terms based on the fit of the model conditional on realizing a significant additive term. Lod score thresholds for each model were empirically derived for a genome-wide significance level of $P<0.05$.

QTL analysis revealed 7 significant and 3 suggestive QTLs for atherosclerosis (Figure 1 and Table 1). Four significant novel QTLs and 1 suggestive novel QTLs were identified and the previously observed *Ath1*, *Athsq1*, *Ath19*, *Ath26*, and *Ath29* loci[15,16,26–28] were replicated. The significant novel QTLs were named according to the standard atherosclerosis QTL nomenclature (*Ath30* to *-33*). Approximately half of the QTLs exhibited codominant heritability, whereas the other half exhibited a dominant effect including *Ath1*, *Athsq1* (males), *Ath19* (females), *Ath26* (females), *Ath31* (females), *Ath33* (female), and chromosome 5, where the lesions of the

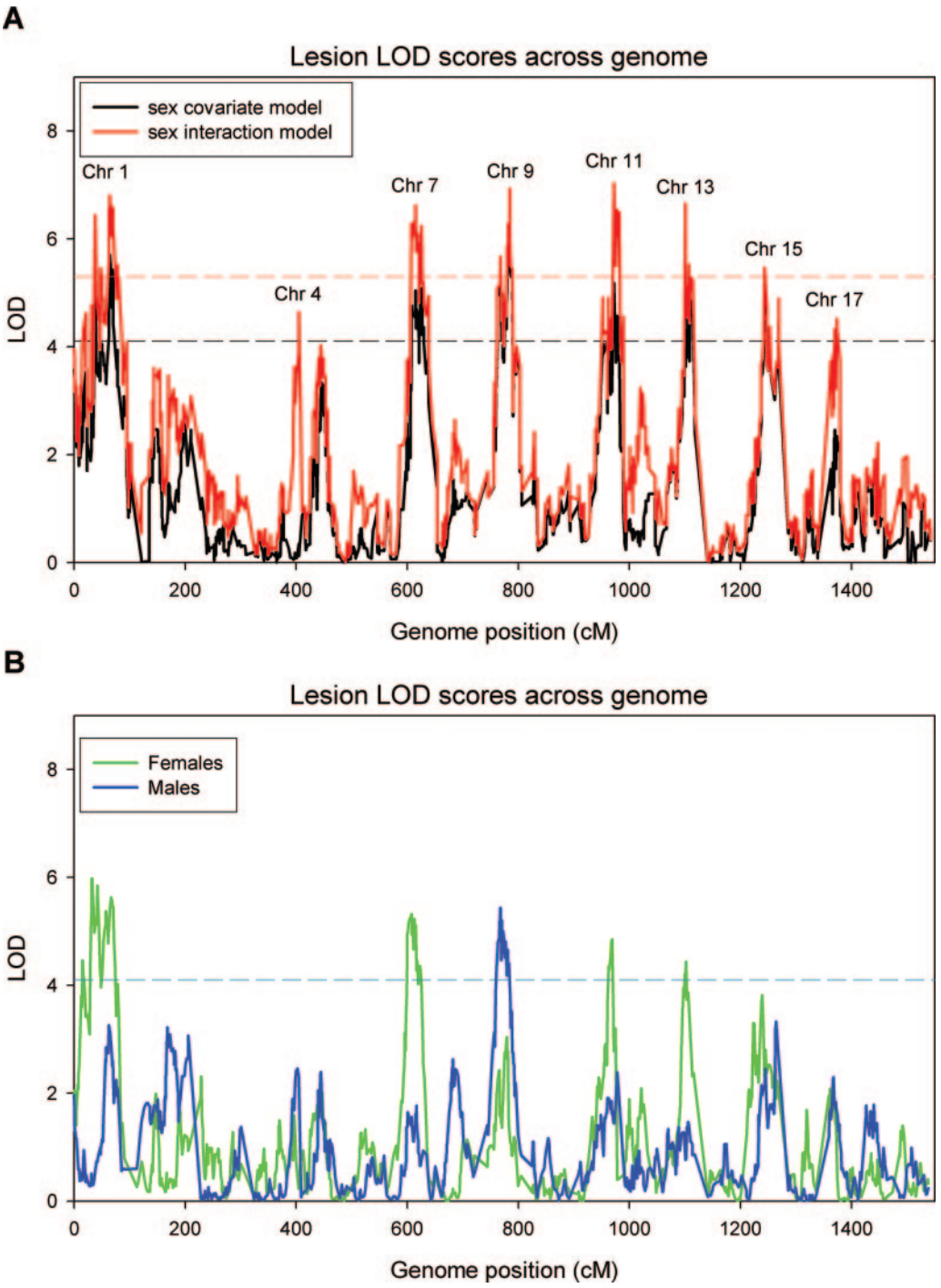

Figure 1. A, All lesion QTLs across the whole genome. QTLs were calculated using sex as a covariate (equation 3, black) and with sex as an interactive covariate (equation 5, red). The dashed red line indicates the genome-wide significance threshold of $P<0.05$ for the model trait$\approx\mu$+add+dom+sex+add·sex+dom·sex (LOD=5.3). The dashed black line indicates the genome-wide significance threshold of $P<0.05$ for the model trait$\approx\mu$+add+dom+sex (LOD=4.1). B, Female (green) and male (blue) QTLs for atherosclerosis across the genome. Additive and dominant contributions were included in the model. The dashed line indicates the genome-wide significance threshold of $P<0.05$ for the model trait$\approx\mu$+add+dom (LOD=4.2).

heterozygotes at these loci were not significantly different from one of the parentals, as assessed by ANOVA (Figure 2). The B6 allele was associated with increased lesion size at 8 of the loci, the C3H allele was associated with increased lesions at 1 locus (*Ath33*) on chromosome 15 and 1 locus on chromosome 4 (*Athsq1*) exhibited opposing associations dependent on sex.

Sex Effects

Sex had a significant effect on lesion development in this cross. The mean female lesion size was 244 524±8694 μm^2, whereas the mean for males was 176 424±7220 μm^2 ($P<0.0001$, SEM t test; Wilcoxon, $P<0.0001$). Individual QTLs demonstrated sex-influenced effects (Figures 2 and 3). Five QTLs were "driven" by females (Figure 1B), whereas

TABLE 1. Suggestive and Significant Lesion QTLs

Locus Name	Chr	SNP Location (Mb)	95% CI (Mb)	SNP ID	LOD (♂+♀)	−log *P* (♂+♀)	LOD (♀)	*P* (♀)	LOD (♂)	*P* (♂)	Allele Effect (♀)	Allele Effect (♂)	High Allele
Ath30	1	76.4	72–80	rs3689327	6.47	5.29	5.98	1.05E-06	0.38	4.17E-01	66 679	17 359	B6
Ath1	1	155.9	135–161	rs3716472	7.08	5.52	5.63	2.34E-06	3.26	5.50E-04	61 719	29 153	B6
Athsq1	4	148.9	145–153	rs3686555	4.97*	3.47	1.59	2.57E-02	2.45	3.55E-03	27 363	24 727	
	5	75.8	65–92	rs3720626	3.99	3.38	2.09	8.13E-03	2.39	4.07E-03	39 037	12 067	B6
Ath31	7	61.7	50–100	rs3677657	6.62	5.12	5.32	4.79E-06	1.56	2.75E-02	53 055	23 013	B6
Ath29	9	84.1	45–89	rs3672897	8.05	6.89	3.04	9.12E-04	4.65	2.24E-05	46 296	44 717	B6
Ath19	11	104.1	64–113	rs3722158	7.76*	5.93	4.85	1.41E-05	2.38	4.17E-03	41 991	34 435	B6
Ath32	13	89.6	86–110	rs3660479	6.93	5.53	4.44	3.63E-05	1.47	3.39E-02	59 608	22 923	B6
Ath33	15	71.4	67–78	rs3696862	6.20	5.26	3.82	1.51E-04	2.45	3.55E-03	40 028	34 313	C3H
Ath26	17	26.1	22–28	rs4231406	4.28*	3.07	1.85	1.41E-02	2.30	5.01E-03	6295	29 047	B6

Chr indicates chromosome; CI, confidence interval; ID, identification no.; ♂, male; ♀, female. *Significant genotype–sex interaction.

males were the main contributors to 1 QTL. *Athsq1*, which was originally identified in a population of F2 females,[26] exhibited "sexual antagonism," (Figure 2) where opposite alleles were associated with increased lesion size dependent on sex. Two sex-specific QTLs were found: *Ath30* was specific for females and *Ath26* for males. Compared with the model accounting for sex as a covariate, the full model improved QTL detection for 3 loci (Table 1), 2 of which, *Athsq1* and *Ath26*, were not detected using the model only accounting for sex as a covariate (Figure 1A). In addition, analyses of the sexes separately only yielded 5 QTLs for females and 1 for males (Figure 1B). Thus, this model selection procedure, accounting for genotype–sex interactions, can identify QTLs that were not detected using previous models.

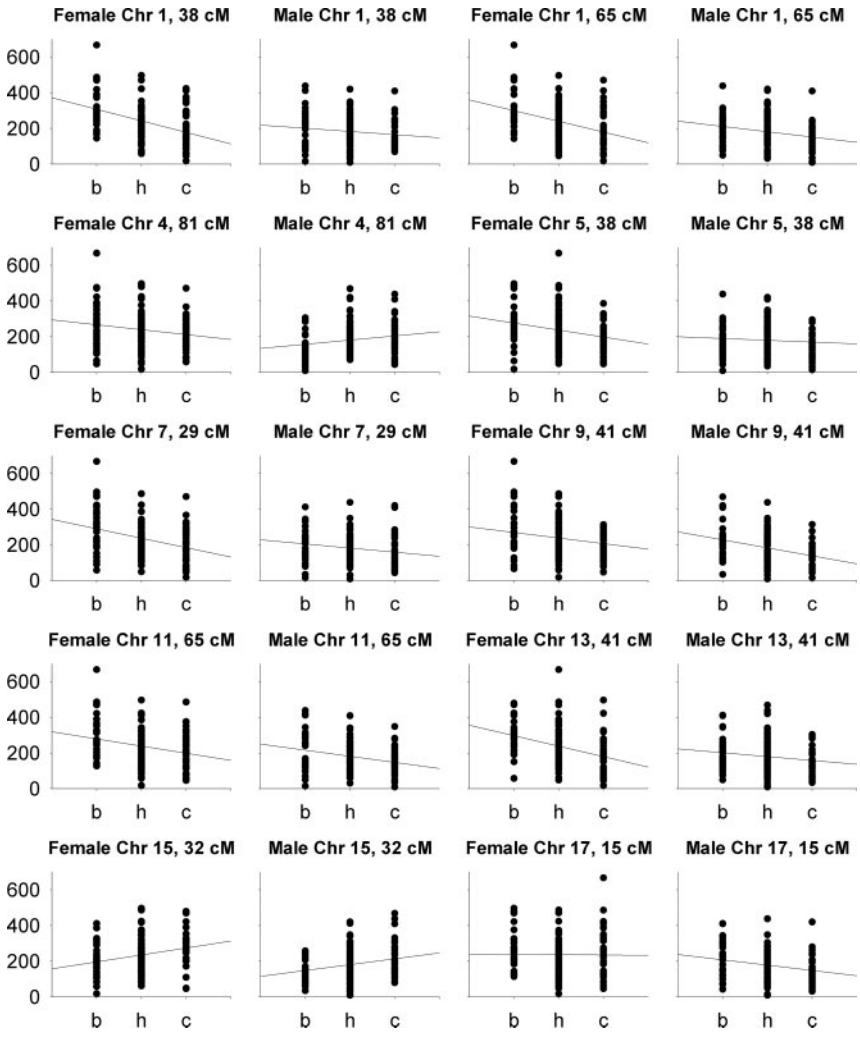

Figure 2. Marker regression for QTL peaks, split by sex. X-axis specifies marker genotypes: b, B6; h, heterozygotes; c, C3H. Y-axis units are aortic lesion area ×1000 μm^2. Each dot represents 1 F2 mouse.

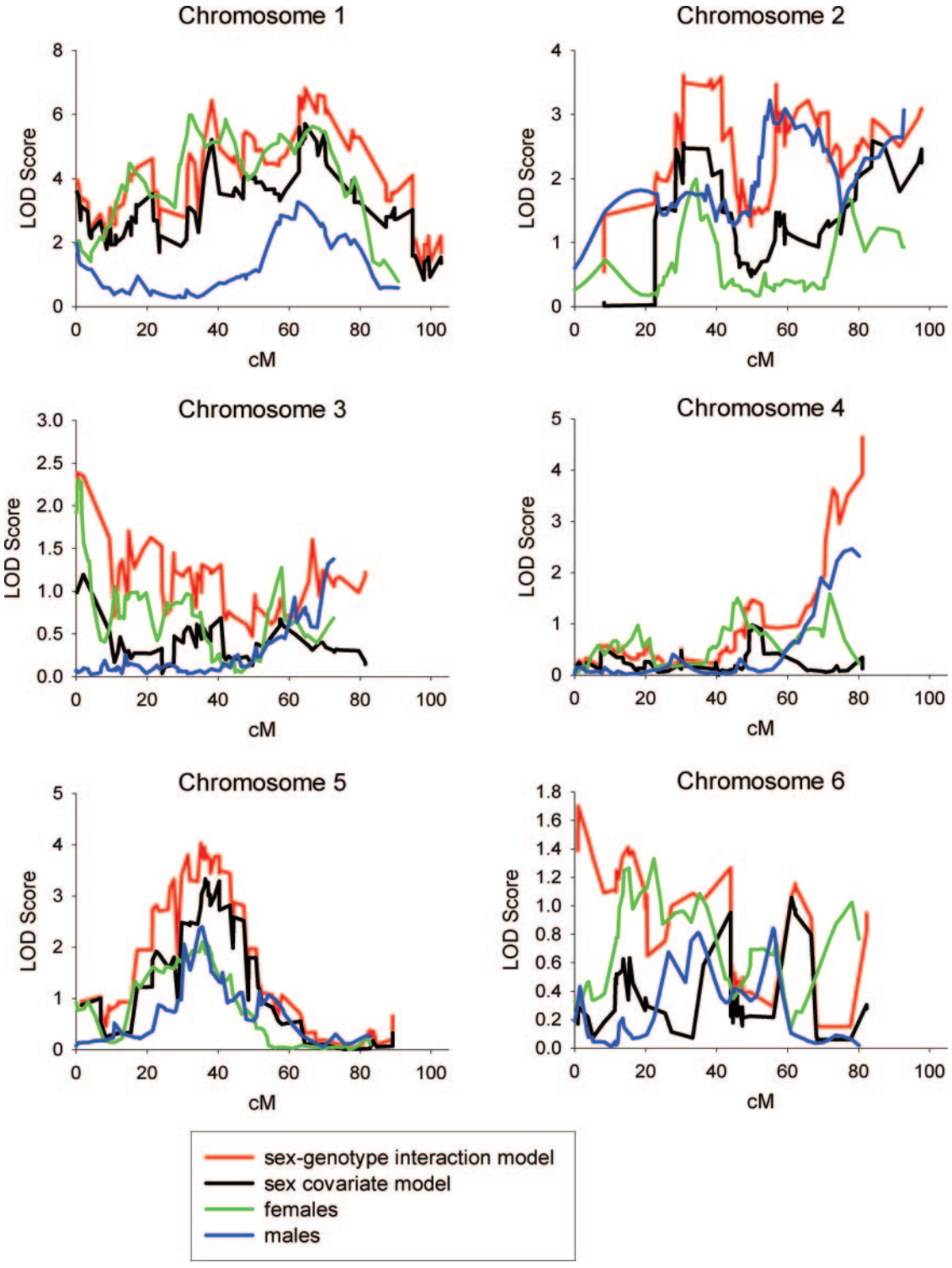

Figure 3. Chromosomal QTL graphs, comparison of QTL models. Red, males and females sex–genotype interaction model; black, males and females sex-covariate model; green, females; blue, males.

Correlations Between Atherosclerosis and Its Various Known Risk Factors

We quantified a variety of risk factors and complications of atherosclerosis to determine their relationship with lesion development in this cross. We performed Pearson correlation incorporating sex as a covariate. The data are summarized in Table 2. Of the traits strongly associated ($P<0.005$), body weight, plasma triglycerides, HDL and insulin were negatively correlated with atherosclerosis, whereas adiposity, plasma glucose to insulin ratio, and adiponectin were positively correlated.

eQTL Approach Reveals Positional Candidate Genes

QTL analysis thus far has identified hundreds of loci for clinical traits but only a handful of genes through positional

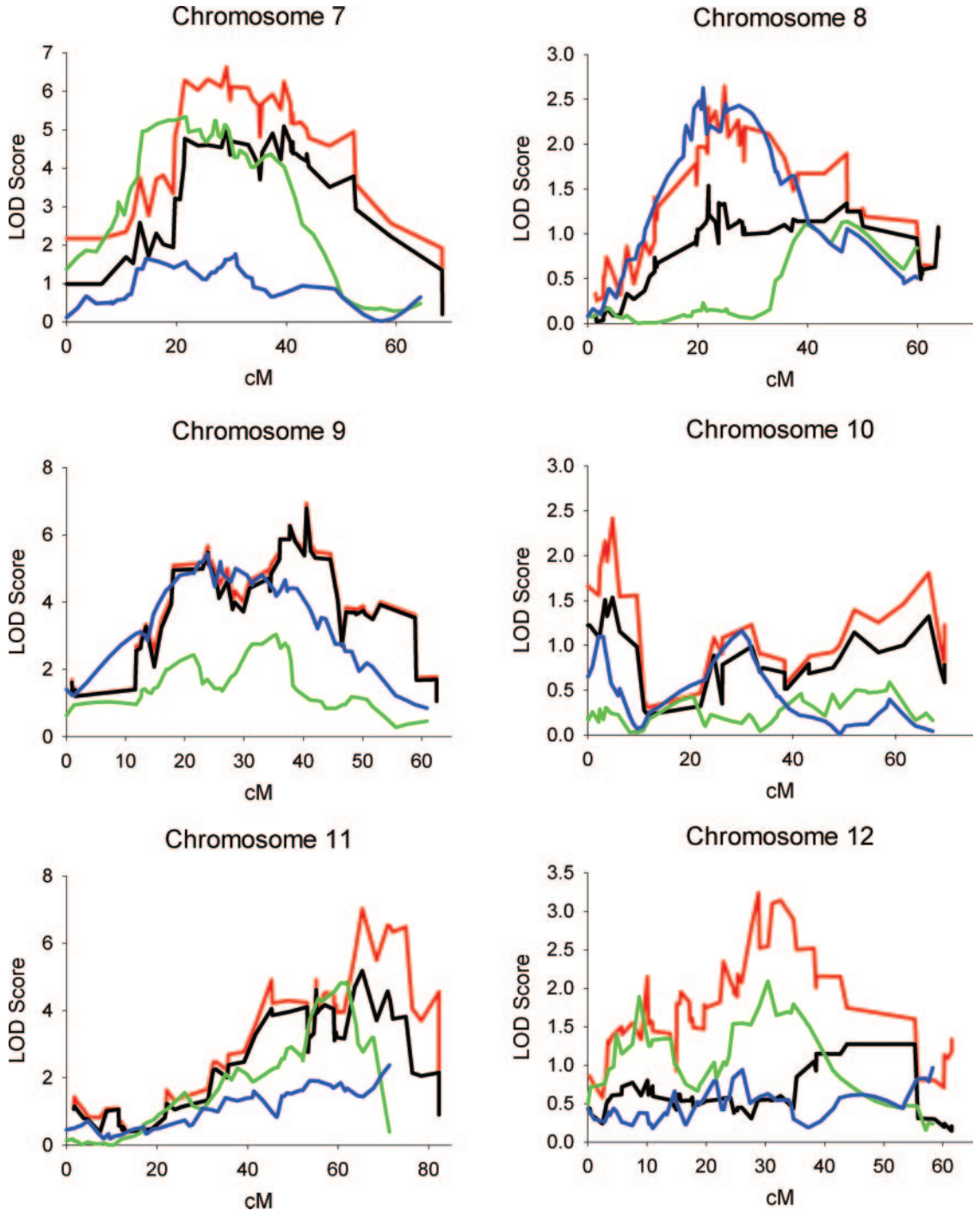

Figure 3. (*Continued*)

cloning.[29] To accelerate the process of identifying genes underlying QTL for complex phenotypes, we performed eQTL analysis using liver and adipose tissue global gene expression data. As discussed below, these tissues were chosen because they are likely to reflect both lipid-related and inflammatory alterations important in atherosclerosis.

A potentially powerful method for the identification of genes underlying QTLs for complex traits is to prioritize the genes based on coincident *cis*-eQTLs. However, because approximately 30% of the significant eQTLs in this cross were *cis*-acting, and because most of the atherosclerosis loci contain hundreds of genes, each of the atherosclerosis loci contain multiple *cis*-eQTLs. Nevertheless, this list should be useful for future work in which the candidates can be tested by transgenic or other experimental procedures. In the liver, 1857 significant eQTLs, representing 1718 genes, colocalized with at least 1 of the 10 atherosclerosis QTLs within 20 Mb (Table I in the online data supplement). Of these, 652 were *cis*- and 1205 were *trans*-eQTLs. In adipose tissue, 1218 significant eQTLs, representing 1142 genes, colocalized with the 10 atherosclerosis cQTLs within 20Mb (supplemental Table II). Of these, 506 were *cis*- and 712 were *trans*-eQTLs.

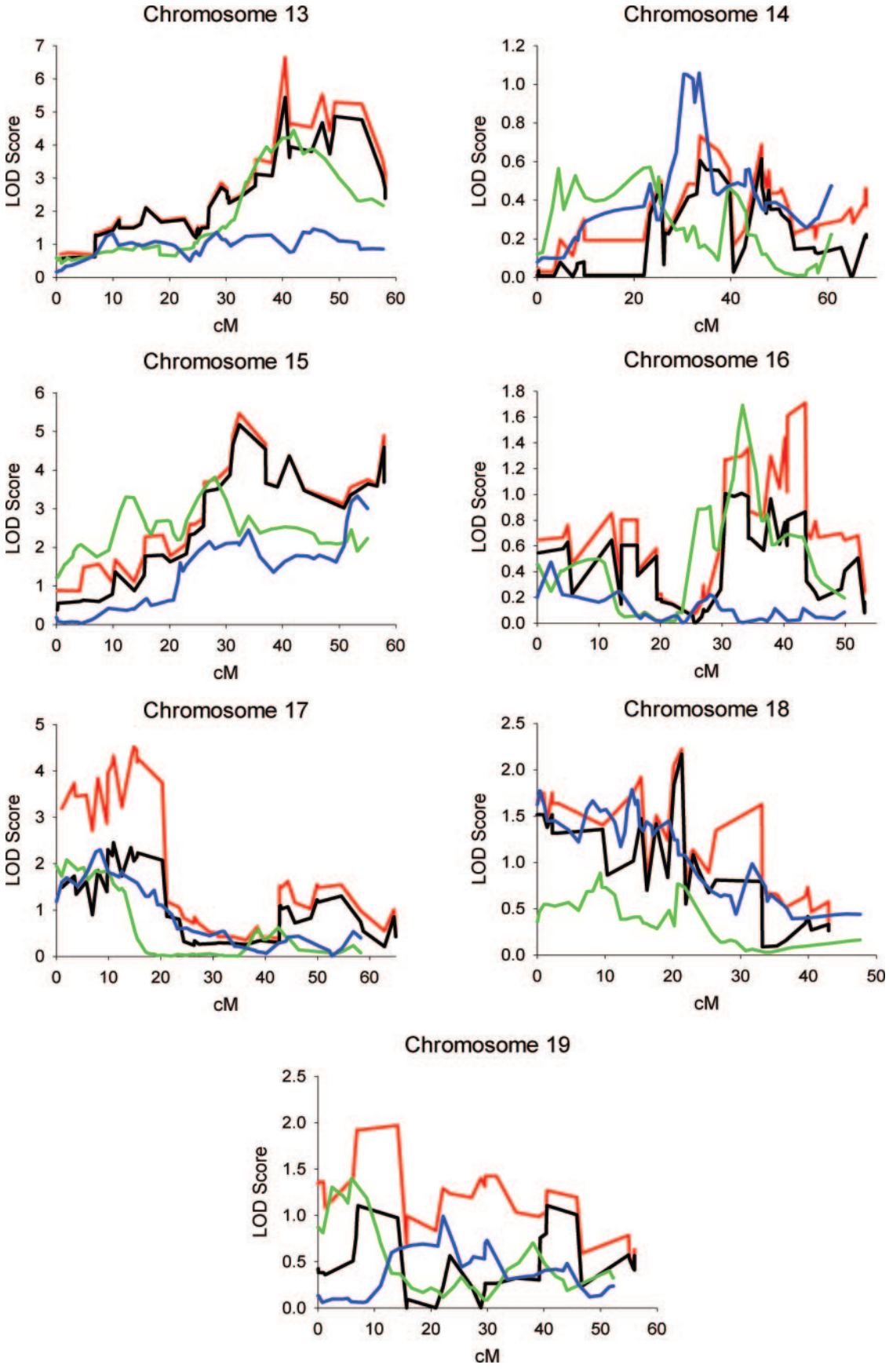

Figure 3. (*Continued*)

TABLE 2. Correlations Between Atherosclerosis and Known Risk Factors and Complications

Trait	R (♂+♀)	P (♂+♀)	R (♂)	P (♂)	R (♀)	P (♀)
Weight	−0.286	1.54E-07	−0.090	0.253	−0.222	0.0045
Abdominal fat	0.112	0.0438	0.095	0.225	−0.117	0.138
Total fat	0.0324	0.561	0.045	0.573	−0.145	0.0664
Adiposity	0.166	0.00290	0.107	0.174	−0.106	0.184
Plasma triglycerides	−0.464	9.39E-19	−0.296	0.0001	−0.342	<0.0001
Plasma total Chol	−0.144	0.00936	−0.099	0.207	−0.131	0.0983
Plasma HDL Chol	−0.282	2.37E-07	−0.172	0.027	−0.203	0.0098
Plasma unesterified Chol	−0.0888	0.110	−0.034	0.661	−0.059	0.461
Plasma free fatty acids	−0.0733	0.188	−0.020	0.804	−0.028	0.721
Plasma glucose	−0.0969	0.0812	−0.079	0.316	−0.091	0.251
Plasma LDL/VLDL Chol	−0.133	0.0166	−0.089	0.255	−0.124	0.120
Plasma MCP-1	−0.144	0.0100	−0.040	0.616	−0.053	0.505
Plasma insulin	−0.305	3.64E-08	−0.125	0.117	−0.155	0.0544
Plasma glucose/insulin	0.313	1.54E-08	0.155	0.0510	0.292	0.0002
Plasma leptin	−0.0206	0.717	0.123	0.126	−0.131	0.105
Plasma adiponectin	0.315	1.99E-08	0.238	0.0031	0.185	0.0221
Hepatic triglycerides	0.0816	0.143	0.177	0.0239	−0.054	0.494
Hepatic total Chol	0.0788	0.158	−0.106	0.181	0.098	0.218
Hepatic unesterified Chol	0.0497	0.373	−0.054	0.492	0.114	0.151

♂ indicates male; ♀, female; Chol, cholesterol; MCP–1, monocyte chemotactic protein 1.

When the sexes were analyzed separately, female liver yielded 453 eQTLs (91 *cis*-, 362 *trans*-) that colocalized with 5 cQTLs (supplemental Table III), and female adipose yielded 553 eQTLs (37 *cis*-, 516 *trans*-) (supplemental Table IV), male liver yielded 32 eQTLs (24 *cis*-, 8 *trans*-) (supplemental Table V), and male adipose yielded 26 eQTLs (24 *cis*-, 2 *trans*-) (supplemental Table VI) that colocalized with 1 QTLs. As discussed below, a powerful approach for the

TABLE 3. Top Ten Genes That Correlate With Atherosclerosis and Have a *Cis*-eQTL Colocalizing With an Atherosclerosis QTL

Tissue and Gene Symbol	Gene Name	Chr	SNP	LOD	R^2	Correlation P
Liver						
Rbp1	Retinol-binding protein 1	9	rs3699740	17.34	0.25	10^{-13}
Bcdo2	β -carotene 9′,10′-dioxygenase 2	9	rs3693234	78.9	0.21	10^{-10}
Plekhb1	Pleckstrin homology domain containing	7	rs3717789	78.2	0.20	10^{-10}
	2310030G06Rik	9	rs3656848	24.0	0.19	10^{-9}
Slc39a4	Solute carrier family 39 A4 (zinc transporter)	15	rs3682805	16.9	0.19	10^{-8}
	A130038L21Rik	13	rs3699802	31.2	0.19	10^{-8}
	2310007B03Rik	1	rs3688242	62.0	0.19	10^{-8}
Blm	Bloom syndrome homolog	7	rs3690268	17.8	0.19	10^{-7}
Anp32a	Acidic (leucine-rich) nuclear phosphoprotein 32 family	9	rs3656848	107.2	0.17	10^{-7}
	5530600A18Rik	11	rs3675440	43.5	0.17	10^{-7}
Adipose						
Igsf4a	Immunoglobulin superfamily, member 4A	9	rs3693351	14.1	0.23	10^{-11}
Cryab	Crystallin αB	9	rs3693234	69.0	0.23	10^{-11}
Iqgap1	IQ motif–containing GTPase-activating protein 1	7	rs3713031	11.8	0.22	10^{-9}
Syngr2	Synaptogyrin 2	11	rs3711884	10.3	0.22	10^{-9}
Hexb	Hexosaminidase B	13	rs3692862	5.9	0.21	10^{-9}
Slc17a5	Solute carrier family 17 A5	9	rs3685573	6.6	0.21	10^{-9}
Anp32a	Acidic (leucine-rich) nuclear phosphoprotein 32 family	9	rs3656848	55.5	0.20	10^{-8}
Csf2rb2	Colony-stimulating factor 2 receptor, β 2	15	rs3667621	5.7	0.21	10^{-8}
Phca	Phytoceramidase, alkaline	7	rs3686975	13.9	0.21	10^{-8}
Ndufc2	NADHP (ubiquinone) 1; subcomplex unknown, 2	7	rs3672246	4.4	0.20	10^{-8}

Chr indicates chromosome.

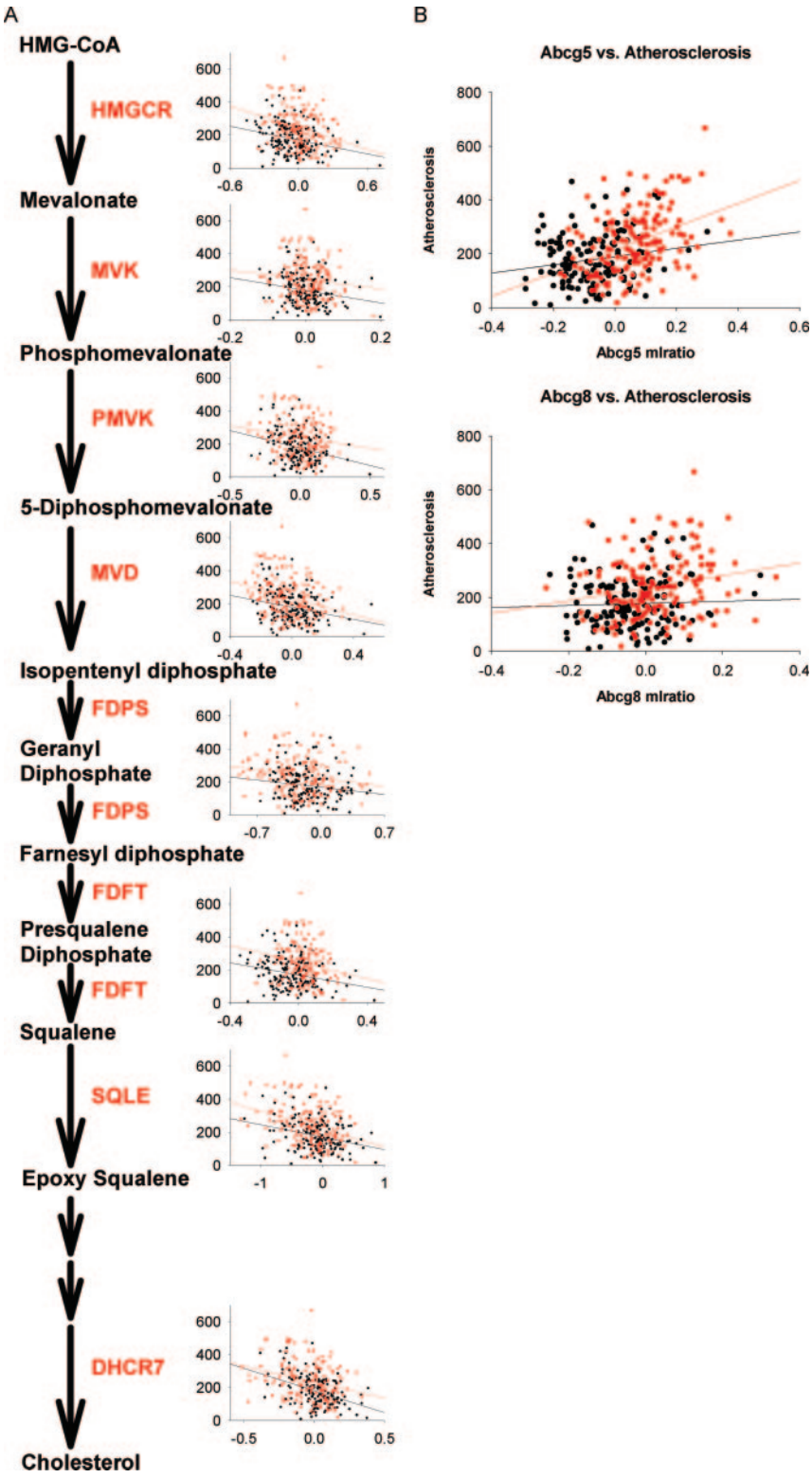

Figure 4. A, The cholesterol biosynthesis pathway is significantly enriched among genes correlated with atherosclerosis in liver. B, *Abcg5* and *Abcg8*, involved in cholesterol excretion into the bile, were also significantly correlated with atherosclerosis. X-axis units are mean log ratio for the gene expression. Y-axis units are aortic lesion area $\times 1000\ \mu m^2$. Each dot represents 1 F2 mouse. Red denotes females; black, males.

identification of both *cis*- and *trans*-acting genes in a complex trait is to use both colocalization and correlation as criteria.

Gene–Trait Correlation and Pathway Analysis

Another method used to select candidate genes was to identify genes whose expression correlated with lesion size. Step-wise regression was used to model the correlation between gene expression and lesion size while using sex as an interactive covariate (equation 7). We identified 1186 genes in liver (supplemental Table VII) and 1950 genes in adipose tissue (supplemental Table VIII) with expression patterns that were correlated with lesion size at a false discovery rate (FDR)<0.01.[30] The overlap between genes with *cis*-eQTLs colocalizing with QTLs and genes correlated with atheroscle-

TABLE 4. Correlations Between Atherosclerosis and Cholesterol Biosynthesis Pathway Gene Expression in Liver

Gene	*R*	*P*	*r* (♀)	*P* (♀)	*r* (♂)	*P* (♂)
Hmgcr	−0.380	5.712×10^{-6}	−0.274	0.000558	−0.258	0.00130
Mvk	−0.367	3.519×10^{-5}	−0.115	0.155	−0.203	0.0120
Pmvk	−0.345	6.463×10^{-4}	−0.143	0.0755	−0.272	0.000660
Mvd	−0.380	7.964×10^{-6}	−0.265	0.000856	−0.257	0.00133
Fdps	−0.348	4.846×10^{-4}	−0.243	0.00254	−0.174	0.0330
Fdft1	−0.344	7.310×10^{-4}	−0.207	0.00975	−0.237	0.00328
Sqle	−0.417	2.100×10^{-8}	−0.345	1.070×10^{-5}	−0.278	6.180×10^{-5}
Dhcr7	−0.421	1.300×10^{-8}	−0.259	0.00112	−0.399	3.219×10^{-7}
Abcg5	−0.400	2.170×10^{-6}	0.370	2.587×10^{-6}	0.179	0.0305
Abcg8	−0.330	0.0185	0.204	0.0111	0.0399	0.624

rosis reduced the list to 135 genes (supplemental Table IX) in liver and 133 genes (supplemental Table X) in adipose tissue for the 10 QTLs. An abbreviated list of candidate genes is presented in Table 3.

When the sexes were analyzed independently, it was found the 1190 genes in female liver were correlated with atherosclerosis (FDR<0.04) (supplemental Table XI) as well as 2167 genes in female adipose (FDR<0.02) (supplemental Table XII), 101 genes in male liver (FDR<0.10) (supplemental Table XIII), and 784 genes in male adipose (FDR<0.10) (supplemental Table XIV). The overlap between *cis*-eQTLs colocalizing with cQTLs and genes correlated with atherosclerosis yielded 103 genes in female liver (supplemental Table XV), 329 genes in female adipose (supplemental Table XVI), 5 genes in male liver (supplemental Table XVII), and 10 genes in male adipose (supplemental Table XVIII). Females had more atherosclerosis cQTLs, more eQTLs overlapping with those cQTLs, and more genes correlated with atherosclerosis than males.

To identify pathways that were related to atherosclerosis in this cross, we subjected the 1186 significantly correlated genes in the liver to pathway analysis using Ingenuity Pathways Analysis (Ingenuity Systems). One canonical pathway was significantly enriched ($P=3.0\times10^{-3}$ as determined by the Fisher exact test after Bonferroni correction): sterol biosynthesis. Eight of the 19 genes in the pathway were correlated with atherosclerosis, and all 8 genes occurred specifically in the cholesterol biosynthesis pathway (Figure 4A and Table 4). They included *Hmgcr*, *Mvk*, *Pmvk*, *Mvd*, *Fdps*, *Fdft1*, *Sqle*, and *Dhcr7*. Because each gene was negatively correlated with atherosclerosis, we hypothesized that cholesterol transport and excretion might also be correlated. We investigated *Abca1*, *Abcg1*, *Abcg5*, and *Abcg8* expression patterns and found that *Abcg5* and *Abcg8* were positively correlated with atherosclerosis (Figure 4B and Table 4). Because the sterol biosynthetic genes were downregulated by cholesterol and the transporters were upregulated, the data suggested that atherosclerosis was associated with increased hepatic cholesterol levels despite the fact that plasma cholesterol levels were negatively correlated with atherosclerosis (Table 2). We subsequently measured hepatic lipid levels and found that hepatic triglycerides were positively correlated with atherosclerosis in males ($P=0.02$). The 8 cholesterol biosynthesis genes mentioned above were each positively correlated with hepatic triglycerides in males (data not shown). However, we did not find that hepatic total or unesterified cholesterol levels were correlated with lesion size.

To identify pathways in adipose tissue, the 1950 adipose tissue genes correlated with atherosclerosis were also subjected to enrichment analysis using Ingenuity Systems. One canonical pathway exhibited a trend toward enrichment: the interleukin (IL)-4 pathway (11 of 36 genes) (Figure 5 and Table 5), and 2 pathways were significantly enriched: the B-cell receptor pathway (29 of 114 genes, $P=1.3\times10^{-2}$) (Figure 6) and oxidative phosphorylation (40 of 139 genes; $P=1.2\times10^{-5}$ after Bonferroni correction) (Figure 7 and Table 6). Most genes in the IL-4 and B-cell receptor pathways were negatively correlated with atherosclerosis, whereas genes comprising complexes I to IV for mitochondrial oxidative phosphorylation were all positively correlated with atherosclerosis. These pathways support a role for inflammatory response and oxidative stress in atherogenesis in this cross.

Discussion

C3H mice are unusually resistant to atherosclerosis and we report here a genetic analysis of a cross between strain C3H and the susceptible strain B6 on the background of hyperlipidemia because of an *ApoE*$^{-/-}$ mutation. The results have led to several conclusions. First, the genetic basis of advanced atherosclerosis in the B6×C3H cross was clearly complex, involving multiple genetic loci. Our work extends prior studies that identified loci on chromosome 1[15] and 9.[16] Second, the development of atherosclerosis in the cross was not only dependent on the sex of the animals but individual loci exhibited different sex-specific effects. Thus, the sex bias observed in our studies indicates that atherosclerosis is caused by a combination of factors that each exhibit sex interactions. Third, we have integrated data for atherosclerosis with whole-genome expression data in this cross to identify pathways involved in atherosclerosis as well as candidate genes. Many of the genes and pathways are novel and several may serve as potential therapeutic targets or new biomarkers. Below we discuss each of these points in turn.

The complexity of atherosclerosis was clearly demonstrated by the identification of 10 QTLs in the BXH *ApoE*$^{-/-}$

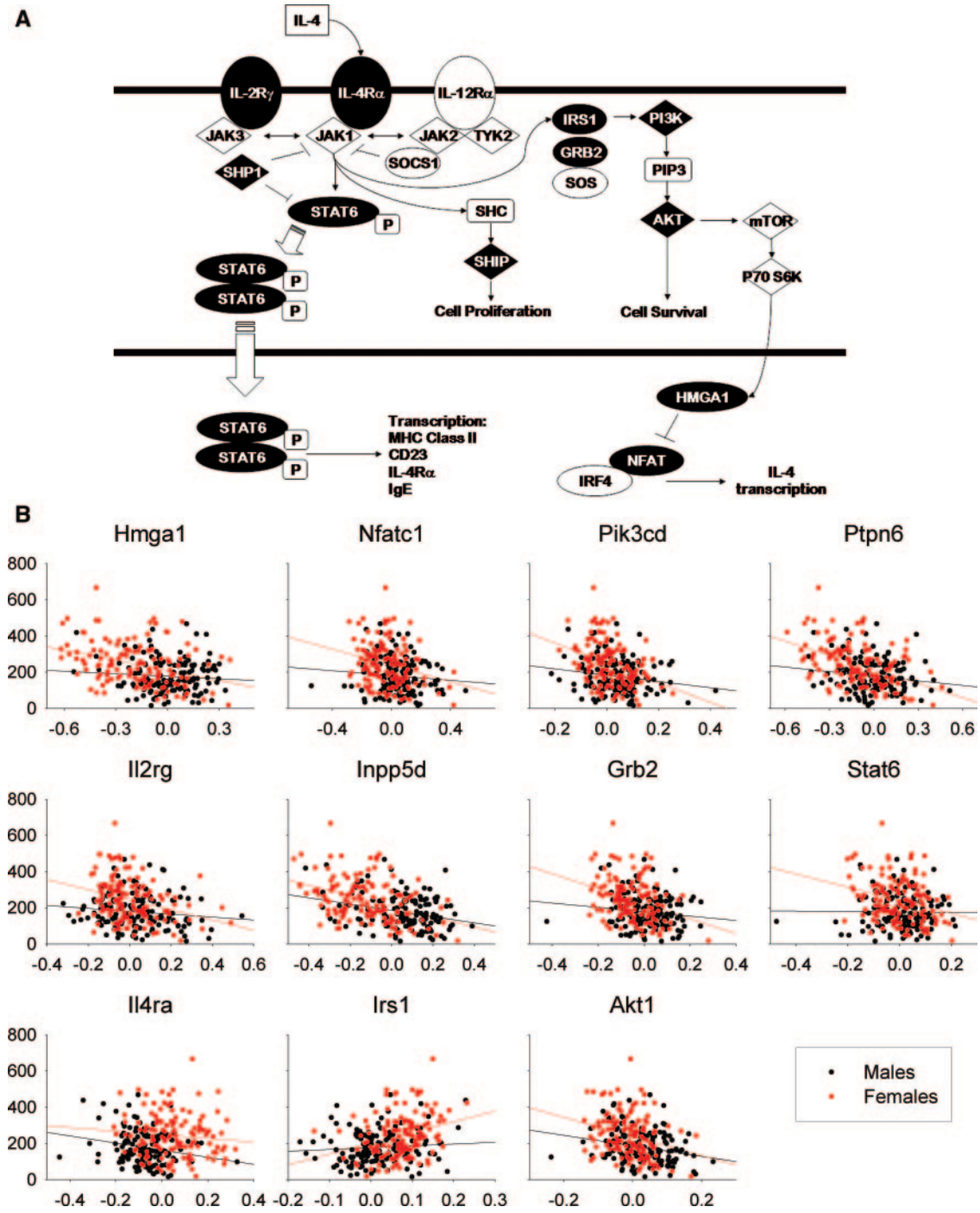

Figure 5. The IL-4 signaling pathway is significantly enriched among genes correlated with atherosclerosis in adipose. A, Genes that are correlated with atherosclerosis are colored in black. Based on KEGG pathways. B, Graphs of the correlations between each individual gene and atherosclerosis ($P<0.001$). X-axis units are mean log ratio for the gene expression. Y-axis units are aortic lesion area $\times 1000\ \mu m^2$. Each dot represents 1 F2 mouse. Red denotes females; black, males.

F2 intercross. Five of the QTLs, *Ath1*, *Athsq1*, *Ath19*, *Ath26*, and *Ath29*, have been previously reported.[15,16,26–28] *Tnfsf4*, which underlies *Ath1*,[31] did not exhibit any liver eQTLs in the cross, although its receptor, *Tnfrsf4*, which is physically located within the 95% confidence interval of *Athsq1* on chromosome 4, has a *cis*-eQTL (LOD=3.39). The fact that *Tnfsf4* did not exhibit a *cis*-eQTL in liver or adipose tissue is not unexpected, as it was shown to be expressed in very low levels in both of these tissues.[31] Although in our experience, the majority of *cis*-eQTLs exhibit a similar genetic perturbation in all tissues in which they are expressed, this is not always the case. Moreover, there are sequence differences in the coding region of the gene between C3H and B6 that may influence function.

A recently published and independently generated cross using the same parental strains and diet obtained 2 QTLs on chromosomes 9 and 11.[16] The discrepancy in the results between Su et al[16] and our cross could be attributable to a

TABLE 5. Correlations Between Atherosclerosis and Interleukin-4 Pathway Gene Expression in Adipose Tissue

Gene	*R*	*P*	*r* (♀)	*P* (♀)	*r* (♂)	*P* (♂)
Shp-1	−0.451	9.09×10^{-9}	−0.425	1.320×10^{-7}	−0.157	0.0553
Il4ra	−0.371	2.77×10^{-4}	−0.141	0.0936	−0.224	0.00590
Pik3cd	−0.392	2.26×10^{-5}	−0.341	1.19910^{-5}	−0.150	0.0664
Irs1	0.383	2.73×10^{-4}	0.294	0.000383	0.0810	0.324
Grb2	−0.391	8.57×10^{-5}	−0.300	0.000286	−0.118	0.149
Akt1	−0.385	3.91×10^{-5}	−0.267	0.00131	−0.219	0.00704
Il2rg	−0.375	8.42×10^{-4}	−0.141	0.0936	−0.129	0.116
Nfatc1	−0.374	9.56×10^{-4}	−0.244	0.00345	−0.101	0.220
Inpp5 days	−0.447	2.18×10^{-9}	−0.372	5.254×10^{-6}	−0.278	0.000560
Stat6	−0.374	8.43×10^{-4}	−0.249	0.00282	−0.0211	0.798
Hmga1	−0.395	5.10×10^{-5}	−0.328	6.930×10^{-5}	−0.0859	0.296

number of factors. Su et al used 234 females, fed the mice on a western diet for 12 weeks starting at 6 weeks of age, and scored lesions by averaging the 5 sections from each mouse with the largest lesions. We generated 334 mice of both sexes, fed them on a western diet for 16 weeks starting at 8 weeks of age, and quantified lesions by averaging 40 evenly distributed sections across the aortic sinus. Both of the differences in the duration of the high-fat diet and the method of lesion quantification could well affect the results. With 50% more mice, our cross was more highly powered to detect QTLs with smaller effects, and the contribution of sex to the genetics of atherosclerotic risk factors has been well documented.[32–34] The age of the mice could also exhibit a significant effect on lesion progression, size, and composition.[35,36] Finally, environmental factors, such as pathogen levels, could also conceivably influence the results. It is noteworthy that 2 surveys of atherosclerosis in different strains of mice fed the "Paigen" diet containing cholic acid, one in a pathogen-free facility and the other in a non–pathogen-free facility, gave strikingly different results.[37] On the other hand, Wright et al did not find an effect of a germ-free environment on atherosclerosis in *ApoE*-null mice.[38]

Because our mice were placed under very strong atherogenic conditions, the QTLs identified may be specific to *ApoE* null hyperlipidemia combined with the feeding of the western diet. The western diet induces some metabolic changes that may or may not be influential on lesion development,[39] and the same mouse cross on a less fatty diet may not exhibit the same QTLs. Another limitation is that we assayed atherosclerosis at 1 site, the aortic sinus. Although aortic sinus lesion areas correlate well with en face quantifications, they cannot account for differences in lesion development in other vascular beds and thus the importance of a specific QTLs for a particular arterial location.[40] Furthermore, the contribution of sex to the different vascular beds cannot be determined. In addition, the pathways identified as correlated to atherosclerosis such as IL-4 may only be relevant to the aortic sinus.[41]

Sex differences in traits and sex-specific QTLs have been previously reported for atherosclerosis[42] and related traits.[18,32,43] The causes of sex differences in susceptibility to atherosclerosis have not been completely elucidated, although sex hormones likely play a role. Our findings clearly show that most of our atherosclerosis QTLs exhibit sex bias, with generally larger effects in females than in males. In mouse studies, females usually develop larger lesions than males, in contrast to the reverse situation in humans. It is also noteworthy that 1 locus exhibits a clear sex interaction, with an allele promoting atherosclerosis in 1 sex and inhibiting it in the other. These sex differences in QTL strength, and the sex specificity of other QTLs, imply that different genes cause atherosclerosis in the 2 sexes, or have different levels of contribution to the disease in the 2 sexes, suggesting that different disease mechanisms are at play. This has significant implications in how we assess genetic risk or treat men and women with the "same" disease.

Using our regression model, there are 2 circumstances under which strong sex-specific QTLs can be obtained. The first is where the trait means of the different QTL genotypes are significantly different between the sexes. The differences in means would result in different QTL strengths for females versus males (given a common variation structure) and would be reflected in the regression, which would have different slopes for the different sexes, and the sex-by-genotype interaction term would thus be significant. The second circumstance where sex-specific QTLs are obtained is when the trait means are the same between males and females when split by genotype, but the variation structure for 1 or more of the genotypes is significantly different between the sexes. This is a situation in which the sex-by-genotype term would not be significant because the interaction term can only assess whether the slopes of the regression lines are different, and in this case, they are identical. Because this situation is not detectable by our model selection procedure, it is valuable to calculate QTLs in the sexes independently of identify sex-specific QTLs of this nature (Figure 1B and 3). For instance, although *Ath30* is a female-specific QTL, the sex-by-genotype term was not significant at this locus (Table 1).

Several traits, either known atherosclerotic risk factors or complications, were correlated with lesion size in this cross. The directions of the correlations for many of these traits are

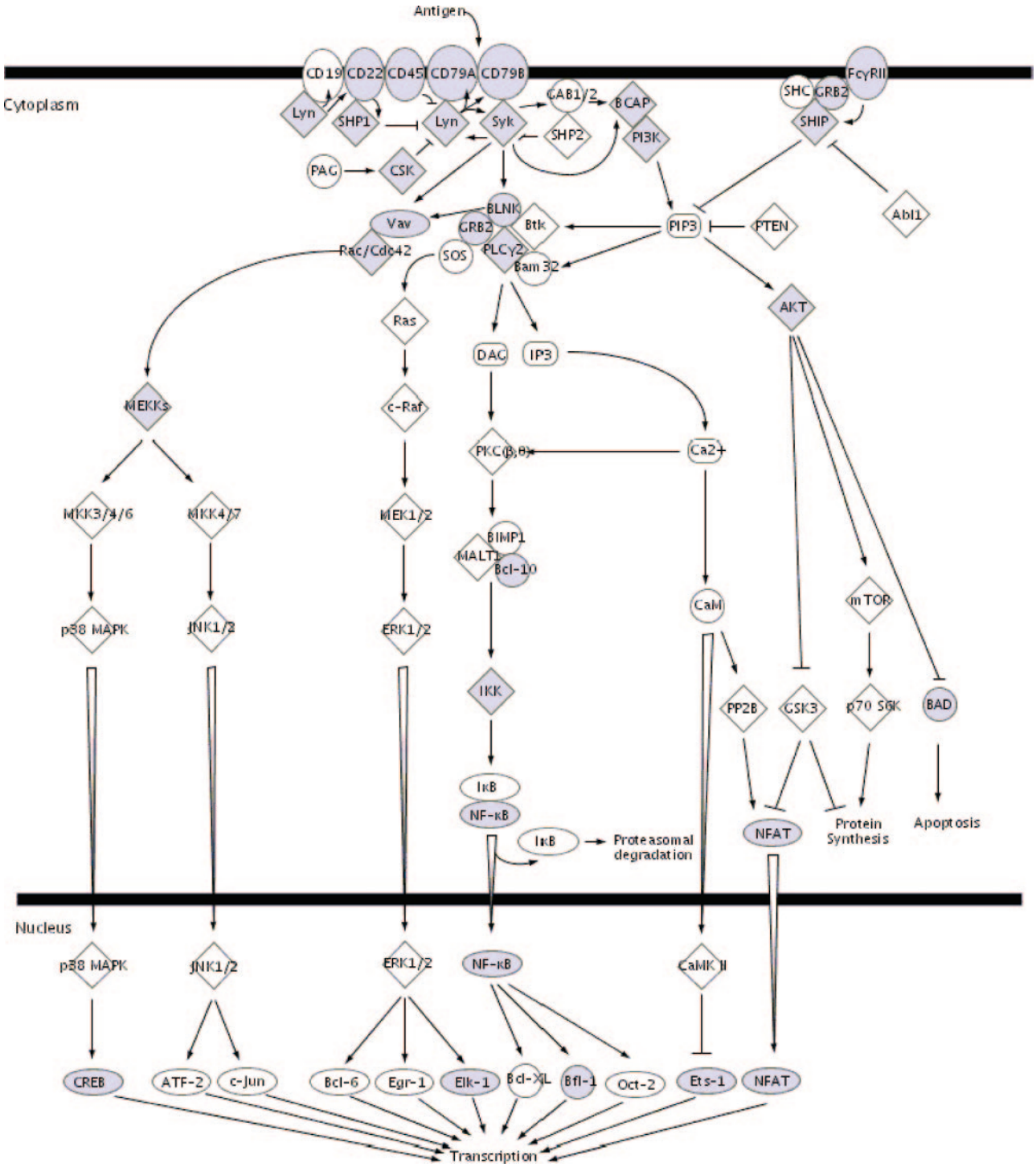

Figure 6. The B-cell receptor signaling pathway is significantly enriched among genes correlated with atherosclerosis in adipose. A, Genes that are correlated with atherosclerosis are colored in gray; courtesy of KEGG pathways. B, Graphs of the correlations between each individual gene and atherosclerosis ($P<0.001$). X-axis units are mean log ratio for the gene expression. Y-axis units are aortic lesion area $\times 1000\ \mu m^2$. Each dot represents one F2 mouse. Red denotes females; black, males.

consistent with epidemiological studies, such as the positive correlations with adiposity and glucose to insulin ratio, and negative correlation with plasma HDL levels. Other traits exhibited correlations in a direction opposite of epidemiological data, such as the negative correlation with plasma triglycerides and the positive correlation with plasma adiponectin levels. The negative correlation with triglycerides could be related to the fact that large triglyceride-rich lipoproteins can be excluded from the vessel wall. We found that the majority of the cholesterol biosynthesis pathway genes in liver were positively correlated with plasma triglyceride and insulin levels and negatively correlated with plasma glucose to insulin ratio and adiponectin levels (data not shown). These traits may be related to lesions through this

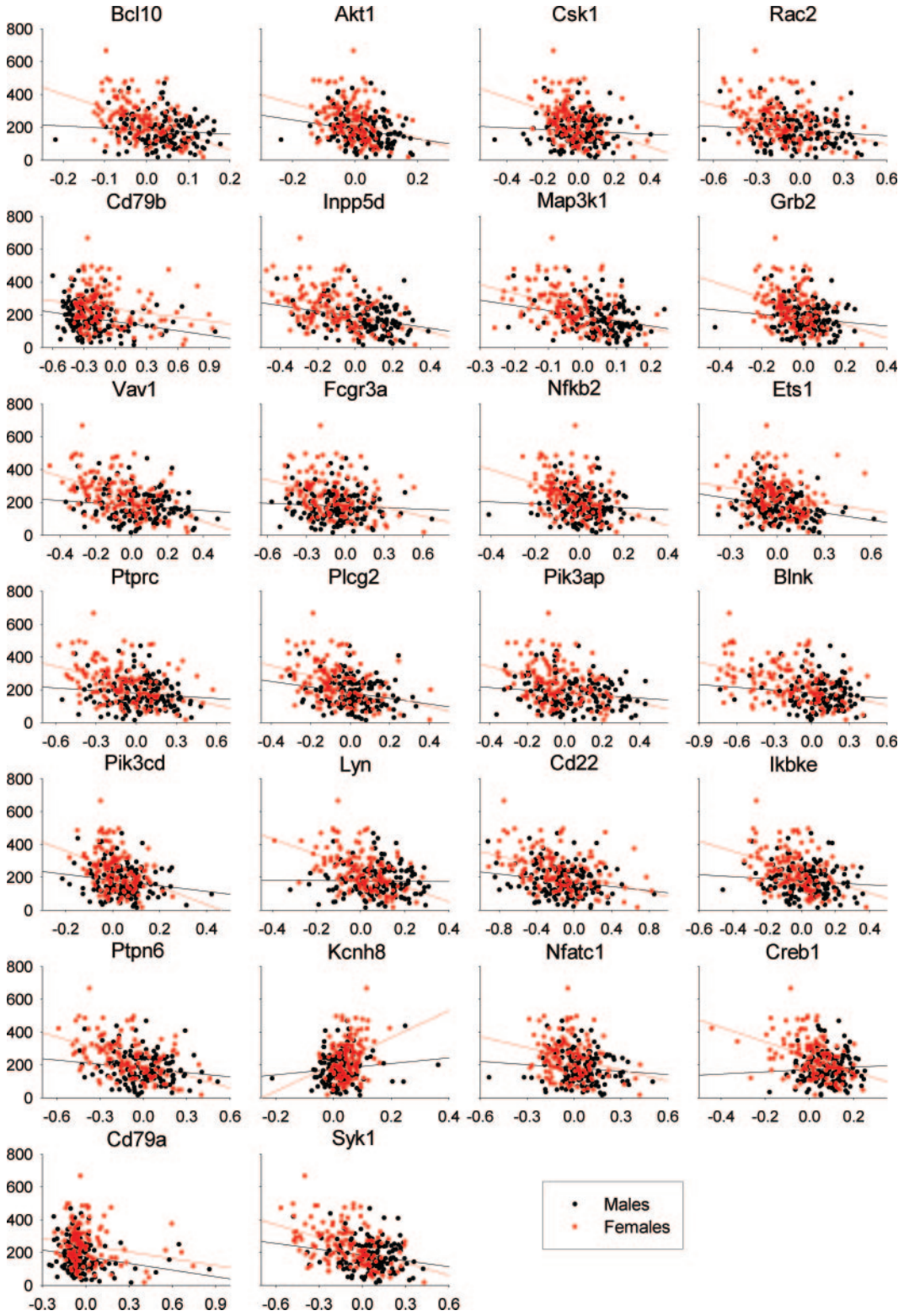

Figure 6. (*Continued*)

pathway. Likewise, many of the genes in the B-cell receptor pathways in adipose tissue were correlated with plasma insulin, leptin, triglycerides, and weight, whereas many genes involved in oxidative phosphorylation were negatively correlated with weight and insulin. Because these traits are associated with insulin resistance and the metabolic syndrome, this cross may be a good model in which to explore the relationships between these traits, pathways, and atherosclerosis.

Several noteworthy genes were included in our list of candidate genes, identified as those with eQTLs colocalizing with lesion QTLs and also correlated with lesion size. For

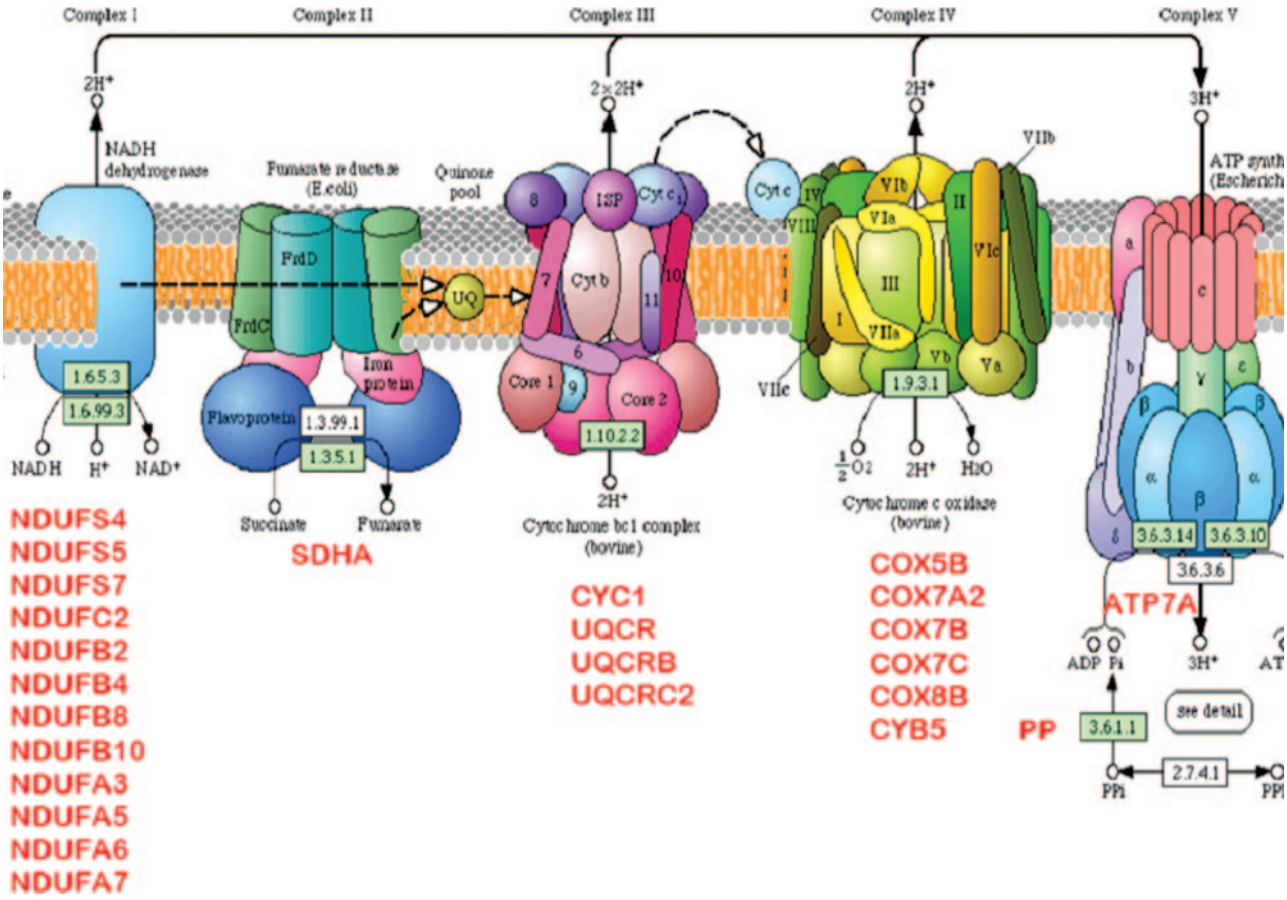

Figure 7. Oxidative phosphorylation is significantly enriched among genes correlated with atherosclerosis in adipose. A, Genes that are correlated with atherosclerosis are denoted in red. Different colors are used to denote individual proteins that make up the subunits of the oxidative phosphorylation complexes; courtesy of KEGG pathways. B, Graphs of the correlations between each individual gene and atherosclerosis ($P<0.001$). X-axis units are mean log ratio for the gene expression. Y-axis units are aortic lesion area $\times 1000\ \mu m^2$. Each dot represents one F2 mouse. Red denotes females; black, males.

example, Stabilin1 (*Stab1*) had 3 eQTLs overlapping with atherosclerosis QTLs and was highly correlated with the trait; it is a prime candidate for atherosclerosis susceptibility with its ability to bind advanced glycation end products and acetylated LDL.[44,45] It is a scavenger receptor that is expressed in liver sinusoidal endothelial cells and macrophages.[46] *Stab1* is not located under any of the lesion QTLs, and thus it must be downstream of the primary perturbing genes. Interleukin 18-binding protein (*Il18bp*), a candidate with 2 overlapping eQTLs, inhibits the binding of IL-18, a cytokine known to promote atherosclerosis in $ApoE^{-/-}$ mice,[47] to its receptor[48] and thereby slows the progression of lesion development and changes the composition of the plaque to a more stable fibrotic phenotype.[49] Moreover, haplotypes of IL-18 have been associated with death from cardiovascular disease in a European population of German nationality.[50] Overall, based on eQTL analysis, we have identified 135 candidate genes in liver and 133 in adipose for 10 atherosclerosis QTLs.

Atherosclerosis clearly alters the cellular composition of the vessel wall, and it would seem to be the most obvious site to evaluate by microarray analyses. However, previous microarray studies of the aorta yielded some inflammatory genes[51] but did not reveal novel genes or pathways responsible for atherogenesis. We chose to study gene expression in liver and adipose tissue because systemic factors associated with these tissues, such as inflammation, hormones, and lipids, clearly influence atherosclerosis or risk factors based on epidemiologic studies. The liver, which consists mostly of hepatocytes but also contains significant numbers of macrophages and other cell types, has long been known to secrete inflammatory molecules. Recently, it has been shown that in mice fed high-fat diets, up to 50% of gonadal fat pad cells are macrophages,[52] a major cell type in atherosclerosis. Thus, we are likely to be directly interrogating the inflammatory state of the animals through both liver and adipose tissue gene expression. Obviously, there are limitations to our study in that some major cell types in atherosclerosis have not been examined. It is also possible that the genes responsible for the disease may not be expressed in the tissues we have studied, or they may not exhibit expression differences or eQTLs. These genes will be missing from this analysis.

Investigation of genes correlated with atherosclerosis revealed that hepatic cholesterol metabolism, inflammation (through the IL-4 and B-cell receptor pathways) and oxidative phosphorylation are likely to play a role in atherogenesis in this cross. The negative correlation between cholesterol metabolism and atherosclerosis was unexpected because

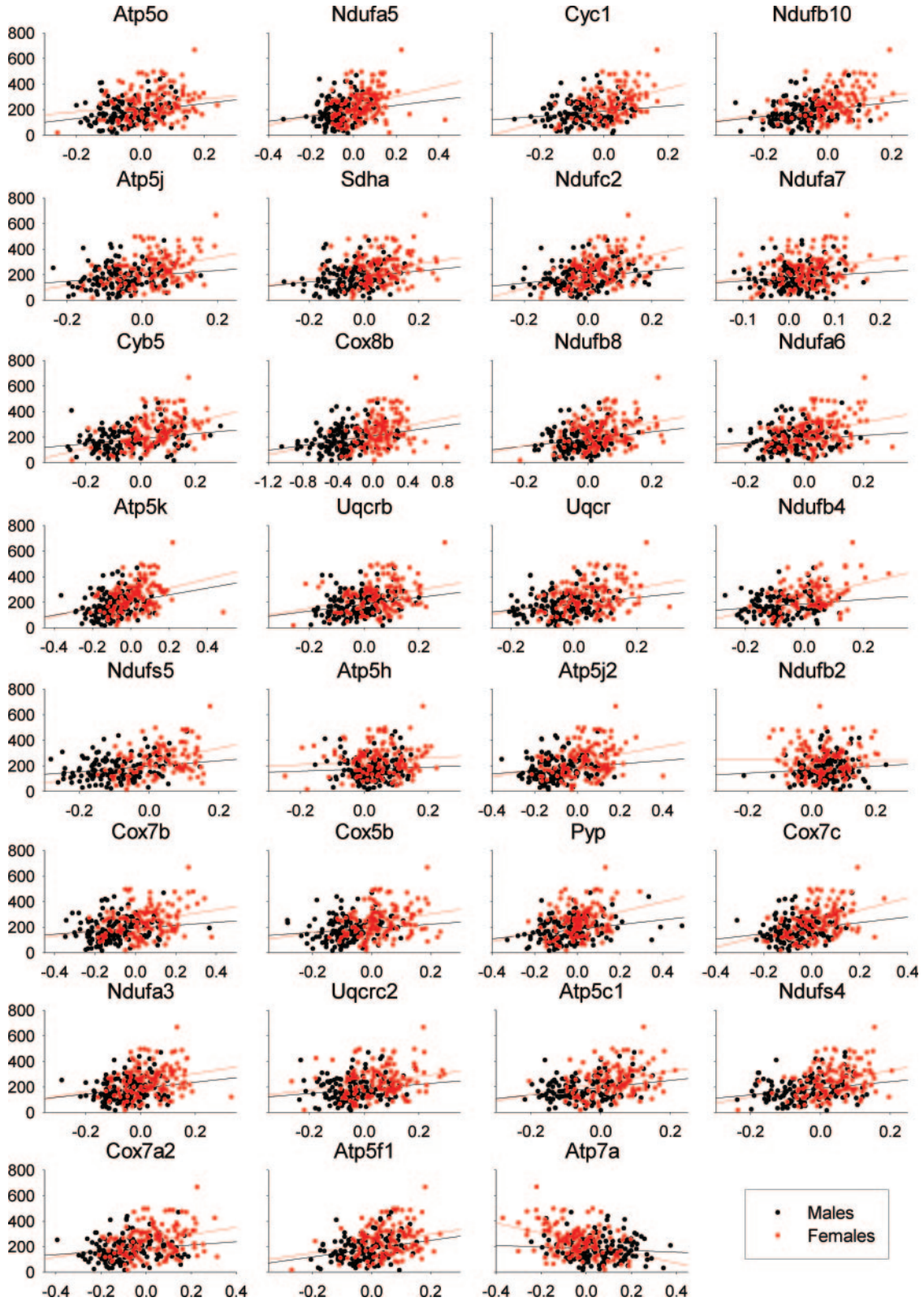

Figure 7. (*Continued*)

plasma cholesterol levels were not associated with atherosclerosis. The IL-4 pathway is known to be both pro- and antiinflammatory[53] as well as prooxidant.[54] The genes in this pathway are negatively correlated with atherosclerosis, which is consistent with an antiinflammatory role. However, IL-4$^{-/-}$;*ApoE*$^{-/-}$ mice exhibited significantly reduced lesions compared with *ApoE*$^{-/-}$ controls, which implicates IL-4 in the promotion of atherosclerosis.[41] In addition, IL-4 has been shown to stimulate reactive oxygen species (ROS) production and macrophage chemotactic protein 1 (*Mcp-1*) expression

TABLE 6. Correlations Between Atherosclerosis and Oxidative Phosphorylation Gene Expression in Adipose Tissue

Gene	*R*	*P*	*r* (♀)	*P* (♀)	*r* (♂)	*P* (♂)
Atp5c1	0.400	4.25×10^{-6}	0.292	0.000656	0.231	0.00615
Atp5f1	0.424	1.14×10^{-6}	0.331	0.000143	0.234	0.00647
Atp5 hours	0.367	4.45×10^{-4}	0.231	0.00575	0.107	0.191
Atp5j	0.417	3.77×10^{-6}	0.343	$3.544\times10^{-5}5$	0.122	0.140
Atp5j2	0.377	5.18×10^{-4}	0.0994	0.239	0.243	0.00269
Atp5k	0.401	2.16×10^{-6}	0.318	0.000151	0.227	0.00589
Atp5o	0.377	1.21×10^{-4}	0.203	0.0156	0.197	0.0157
Atp7a	0.405	1.21×10^{-5}	−0.361	1.018×10^{-5}	−0.0575	0.485
Pyp	0.416	2.82×10^{-5}	0.233	0.00555	0.267	0.00198
Cox5b	0.363	7.72×10^{-4}	0.261	0.00183	0.125	0.124
Cox7a2	0.387	1.69×10^{-4}	0.297	0.000328	0.136	0.0957
Cox7b	0.379	4.25×10^{-4}	0.306	0.000402	0.118	0.150
Cox7c	0.439	7.74×10^{-8}	0.391	2.998×10^{-6}	0.178	0.0305
Cox8b	0.370	3.12×10^{-4}	0.255	0.00233	0.243	0.00256
Cyb5	0.442	5.01×10^{-8}	0.397	1.079×10^{-6}	0.216	0.00783
Cyc1	0.436	2.09×10^{-5}	0.389	1.229×10^{-5}	0.141	0.108
Uqcr	0.415	3.76×10^{-6}	0.335	4.791×10^{-5}	0.183	0.0252
Uqcrb	0.422	1.49×10^{-7}	0.361	1.163×10^{-5}	0.227	0.00540
Uqcrc2	0.366	6.14×10^{-4}	0.224	0.00741	0.122	0.138
Sdha	0.362	9.63×10^{-4}	0.210	0.0121	0.166	0.0428
Ndufa3	0.377	1.36×10^{-4}	0.254	0.00225	0.172	0.0351
Ndufa5	0.374	9.71×10^{-4}	0.269	0.00137	0.0648	0.431
Ndufa6	0.391	9.20×10^{-5}	0.294	0.000385	0.0907	0.271
Ndufa7	0.363	7.99×10^{-4}	0.246	0.00311	0.115	0.162
Ndufb10	0.392	4.35×10^{-5}	0.248	0.00475	0.211	0.0113
Ndufb2	0.394	1.18×10^{-5}	0.302	0.000275	0.201	0.0137
Ndufb4	0.447	1.95×10^{-5}	0.400	2.629×10^{-5}	0.142	0.119
Ndufb8	0.397	6.21×10^{-6}	0.320	0.000128	0.162	0.0456
Ndufs4	0.402	2.92×10^{-6}	0.297	0.000327	0.226	0.00538
Ndufs5	0.416	2.96×10^{-5}	0.351	0.0000958	0.163	0.0562
Ndufs7	0.366	5.17×10^{-4}	0.264	0.00151	0.124	0.129
Ndufc2	0.452	7.53×10^{-9}	0.423	1.627×10^{-7}	0.205	0.0120

and to inhibit nitric oxide bioavailability in endothelial cells.[55]

The positive correlation between components of complexes I to IV in oxidative phosphorylation and atherosclerosis suggests a role for mitochondrial ROS in lesion formation. Mitochondrial respiration results in the generation of ROS such as superoxide and hydrogen peroxide.[56] The positive correlation between the proton electrochemical gradient and ROS production is attributable to the inhibition of electron flow down the electron transport chain, which prolongs the half-life of the intermediates capable of reducing oxygen to superoxide. ROS production can be reduced by uncoupling reagents and proteins that decrease the electrochemical gradient.[57] Superoxide activates uncoupling proteins indirectly through lipid peroxidation products and reactive aldehydes. We found that uncoupling protein 2 (*Ucp2*) expression in the gonadal fat pad was negatively correlated with atherosclerosis in this cross (supplemental Table VIII). *Ucp2* expression in macrophages protects against atherosclerosis on the $Ldlr^{-/-}$ background.[58] The mechanism proposed is that *Ucp2* reduces oxidative stress by promoting the "leakage" of protons across the mitochondrial membrane, thereby reducing membrane potential and superoxide production. A deficiency of *Ucp2* in macrophages was associated with increased macrophage content, apoptosis, and nitrotyrosine staining (an indicator of oxidative stress), and decreased collagen content in lesions, which is consistent with a more vulnerable plaque. This supports the hypothesis that mitochondrial damage and dysfunction are major contributors to the development of cardiovascular disease.[57] These changes in adipose tissue may affect atherosclerosis in multiple ways. One hypothesis is that macrophages in adipose tissue are reflective of macrophages in the atherosclerotic lesion. Alternatively, macrophages may influence adipose tissue function, which in turn affects atherosclerosis. In addition, because genes involved in energy metabolism

emerged as an important functional group, mitochondria-encoded genes, and thus maternal-specific inheritance, may also play a role in atherosclerosis as they also contribute to energy metabolism.

The integration of expression and trait data in a segregating cross provides a powerful tool for the identification of genes and pathways involved in complex traits. Our data support the involvement of specific inflammatory pathways and mitochondrial oxidative stress in atherosclerosis and also provide a list of novel candidate genes. They also reveal a connection between global gene expression in the liver and adipose tissue with atherosclerosis. Identifying pathways relevant to atherosclerosis in these tissues and potential pathway interrelationships suggests that we can track systemic processes affecting lesion development in peripheral tissues.

Acknowledgments

We thank Sarada Charugundla for performing the lipid assays; Anatole Ghazalpour, Shristi Regmi, Iche Siah, and Leandra Velky for assisting in tissue homogenization; Richard Davis, Anatole Ghazalpour, Sudheer Doss, Carmen Zelaya, Hannah Qi, Judy Wu, Pingzi Wen, Zory Shaposhnik, Yishou Shi, and Soumya Chari for assistance in euthanizing the animals; Sonia Carlson for her organization of the transfer tissues and data between institutions; and Nadir Yehya, Peter Gargalovic, Parthive Patel, and Xia Yang for valuable discussion and insight.

Sources of Funding

This work was supported by NIH grants HL30568 (to A.J.L. and T.A.D.) and HL28481 (to A.J.L.); Public Health Service training grant HD07228-24 (to S.S.W.); and the Iris Cantor–University of California at Los Angeles Women's Health Center, University of California at Los Angeles National Center for Excellence in Women's Health (to T.A.D.). Genotyping was supported by the National Heart, Lung, and Blood Institute Mammalian Genotyping Service (contract no. HV48141 to S.S.W.).

Disclosures

None.

References

1. Lusis AJ, Mar R, Pajukanta P. Genetics of atherosclerosis. *Annu Rev Genomics Hum Genet*. 2004;5:189–218.
2. Allayee H, Ghazalpour A, Lusis AJ. Using mice to dissect genetic factors in atherosclerosis. *Arterioscler Thromb Vasc Biol*. 2003;23:1501–1509.
3. Wang X, Ishimori N, Korstanje R, Rollins J, Paigen B. Identifying novel genes for atherosclerosis through mouse-human comparative genetics. *Am J Hum Genet*. 2005;77:1–15.
4. Schadt EE, Monks SA, Drake TA, Lusis AJ, Che N, Colinayo V, Ruff TG, Milligan SB, Lamb JR, Cavet G, Linsley PS, Mao M, Stoughton RB, Friend SH. Genetics of gene expression surveyed in maize, mouse and man. *Nature*. 2003;422:297–302.
5. Chesler EJ, Lu L, Shou S, Qu Y, Gu J, Wang J, Hsu HC, Mountz JD, Baldwin NE, Langston MA, Threadgill DW, Manly KF, Williams RW. Complex trait analysis of gene expression uncovers polygenic and pleiotropic networks that modulate nervous system function. *Nat Genet*. 2005;37:233–242.
6. Bystrykh L, Weersing E, Dontje B, Sutton S, Pletcher MT, Wiltshire T, Su AI, Vellenga E, Wang J, Manly KF, Lu L, Chesler EJ, Alberts R, Jansen RC, Williams RW, Cooke MP, de Haan G. Uncovering regulatory pathways that affect hematopoietic stem cell function using 'genetical genomics'. *Nat Genet*. 2005;37:225–232.
7. Hubner N, Wallace CA, Zimdahl H, Petretto E, Schulz H, Maciver F, Mueller M, Hummel O, Monti J, Zidek V, Musilova A, Kren V, Causton H, Game L, Born G, Schmidt S, Muller A, Cook SA, Kurtz TW, Whittaker J, Pravenec M, Aitman TJ. Integrated transcriptional profiling and linkage analysis for identification of genes underlying disease. *Nat Genet*. 2005;37:243–253.
8. Doss S, Schadt EE, Drake TA, Lusis AJ. Cis-acting expression quantitative trait loci in mice. *Genome Res*. 2005;15:681–691.
9. Yaguchi H, Togawa K, Moritani M, Itakura M. Identification of candidate genes in the type 2 diabetes modifier locus using expression QTL. *Genomics*. 2005;85:591–599.
10. Yamashita S, Wakazono K, Nomoto T, Tsujino Y, Kuramoto T, Ushijima T. Expression quantitative trait loci analysis of 13 genes in the rat prostate. *Genetics*. 2005;171:1231–1238.
11. Palmer AA, Verbitsky M, Suresh R, Kamens HM, Reed CL, Li N, Burkhart-Kasch S, McKinnon CS, Belknap JK, Gilliam TC, Phillips TJ. Gene expression differences in mice divergently selected for methamphetamine sensitivity. *Mamm Genome*. 2005;16:291–305.
12. MacLaren EJ, Sikela JM. Cerebellar gene expression profiling and eQTL analysis in inbred mouse strains selected for ethanol sensitivity. *Alcohol Clin Exp Res*. 2005;29:1568–1579.
13. Schadt EE, Lamb J, Yang X, Zhu J, Edwards S, Guhathakurta D, Sieberts SK, Monks S, Reitman M, Zhang C, Lum PY, Leonardson A, Thieringer R, Metzger JM, Yang L, Castle J, Zhu H, Kash SF, Drake TA, Sachs A, Lusis AJ. An integrative genomics approach to infer causal associations between gene expression and disease. *Nat Genet*. 2005;37:710–717.
14. Plump AS, Smith JD, Hayek T, Aalto-Setala K, Walsh A, Verstuyft JG, Rubin EM, Breslow JL. Severe hypercholesterolemia and atherosclerosis in apolipoprotein E-deficient mice created by homologous recombination in ES cells. *Cell*. 1992;71:343–353.
15. Paigen B, Mitchell D, Reue K, Morrow A, Lusis AJ, LeBoeuf RC. Ath-1, a gene determining atherosclerosis susceptibility and high density lipoprotein levels in mice. *Proc Natl Acad Sci U S A*. 1987;84:3763–3767.
16. Su Z, Li Y, James JC, McDuffie M, Matsumoto AH, Helm GA, Weber JL, Lusis AJ, Shi W. Quantitative trait locus analysis of atherosclerosis in an intercross between C57BL/6 and C3H mice carrying the mutant apolipoprotein E gene. *Genetics*. 2006;172:1799–1807.
17. Shi W, Wang NJ, Shih DM, Sun VZ, Wang X, Lusis AJ. Determinants of atherosclerosis susceptibility in the C3H and C57BL/6 mouse model: evidence for involvement of endothelial cells but not blood cells or cholesterol metabolism. *Circ Res*. 2000;86:1078–1084.
18. Wang S, Yehya N, Schadt EE, Wang H, Drake TA, Lusis AJ. Genetic and genomic analysis of a fat mass trait with complex inheritance reveals marked sex specificity. *PLoS Genet*. 2006;2:e15.
19. Ghazalpour A, Doss S, Zhang B, Wang S, Plaisier C, Castellanos R, Brozell A, Schadt EE, Drake TA, Lusis AJ, Horvath S. Integrating genetic and network analysis to characterize genes related to mouse weight. *PLoS Genet*. 2006;2:e130.
20. Yang X, Schadt EE, Wang S, Wang H, Arnold AP, Ingram-Drake L, Drake TA, Lusis AJ. Tissue-specific expression and regulation of sexually dimorphic genes in mice. *Genome Res*. 2006;16:995–1004.
21. Mehrabian M, Qiao JH, Hyman R, Ruddle D, Laughton C, Lusis AJ. Influence of the apoA-II gene locus on HDL levels and fatty streak development in mice. *Arterioscler Thromb*. 1993;13:1–10.
22. Hardenbol P, Baner J, Jain M, Nilsson M, Namsaraev EA, Karlin-Neumann GA, Fakhrai-Rad H, Ronaghi M, Willis TD, Landegren U, Davis RW. Multiplexed genotyping with sequence-tagged molecular inversion probes. *Nat Biotechnol*. 2003;21:673–678.
23. Lander E, Kruglyak L. Genetic dissection of complex traits: guidelines for interpreting and reporting linkage results. *Nat Genet*. 1995;11:241–247.
24. Wang S, Basten CJ, Zeng ZB. *Windows QTL Cartographer*, version 2.5. Raleigh, NC: Department of Statistics, North Carolina State University; 2006 Available at http://statgen.ncsu.edu/qtlcart/WQTLCart.htm.
25. He YD, Dai H, Schadt EE, Cavet G, Edwards SW, Stepaniants SB, Duenwald S, Kleinhanz R, Jones AR, Shoemaker DD, Stoughton RB. Microarray standard data set and figures of merit for comparing data processing methods and experiment designs. *Bioinformatics*. 2003;19:956–965.
26. Welch CL, Bretschger S, Latib N, Bezouevski M, Guo Y, Pleskac N, Liang CP, Barlow C, Dansky H, Breslow JL, Tall AR. Localization of atherosclerosis susceptibility loci to chromosomes 4 and 6 using the Ldlr knockout mouse model. *Proc Natl Acad Sci U S A*. 2001;98:7946–7951.
27. Ishimori N, Li R, Kelmenson PM, Korstanje R, Walsh KA, Churchill GA, Forsman-Semb K, Paigen B. Quantitative trait loci analysis for plasma HDL-cholesterol concentrations and atherosclerosis susceptibility between inbred mouse strains C57BL/6J and 129S1/SvImJ. *Arterioscler Thromb Vasc Biol*. 2004;24:161–166.
28. Smith JD, Bhasin JM, Baglione J, Settle M, Xu Y, Barnard J. Atherosclerosis susceptibility loci identified from a strain intercross of apoli-

poprotein E-deficient mice via a high-density genome scan. *Arterioscler Thromb Vasc Biol*. 2006;26:597–603.
29. Flint J, Valdar W, Shifman S, Mott R. Strategies for mapping and cloning quantitative trait genes in rodents. *Nat Rev Genet*. 2005;6:271–286.
30. Benjamini Y, Hochberg Y. Controlling the false discovery rate: a practical and powerful approach to multiple testing. *J R Stat Soc Ser B Stat Soc*. 1995;57:289–300.
31. Wang X, Ria M, Kelmenson PM, Eriksson P, Higgins DC, Samnegard A, Petros C, Rollins J, Bennet AM, Wiman B, de Faire U, Wennberg C, Olsson PG, Ishii N, Sugamura K, Hamsten A, Forsman-Semb K, Lagercrantz J, Paigen B. Positional identification of TNFSF4, encoding OX40 ligand, as a gene that influences atherosclerosis susceptibility. *Nat Genet*. 2005;37:365–372.
32. Korstanje R, Li R, Howard T, Kelmenson P, Marshall J, Paigen B, Churchill G. Influence of sex and diet on quantitative trait loci for HDL cholesterol levels in an SM/J by NZB/BlNJ intercross population. *J Lipid Res*. 2004;45:881–888.
33. Avery CL, Freedman BI, Kraja AT, Borecki IB, Miller MB, Pankow JS, Arnett D, Lewis CE, Myers RH, Hunt SC, North KE. Genotype-by-sex interaction in the aetiology of type 2 diabetes mellitus: support for sex-specific quantitative trait loci in Hypertension Genetic Epidemiology Network participants. *Diabetologia*. 2006;49:2329–2336.
34. Franceschini N, MacCluer JW, Goring HH, Cole SA, Rose KM, Almasy L, Diego V, Laston S, Lee ET, Howard BV, Best LG, Fabsitz RR, Roman MJ, North KE. A quantitative trait loci-specific gene-by-sex interaction on systolic blood pressure among American Indians: the Strong Heart Family Study. *Hypertension*. 2006;48:266–270.
35. Nakashima Y, Plump AS, Raines EW, Breslow JL, Ross R. ApoE-deficient mice develop lesions of all phases of atherosclerosis throughout the arterial tree. *Arterioscler Thromb*. 1994;14:133–140.
36. Reddick RL, Zhang SH, Maeda N. Atherosclerosis in mice lacking apo E. Evaluation of lesional development and progression. *Arterioscler Thromb*. 1994;14:141–147.
37. Bogue MA, Grubb SC, Maddatu TP, Bult CJ. Mouse Phenome Database (MPD). *Nucleic Acids Res*. 2007;35:D643–D649.
38. Wright SD, Burton C, Hernandez M, Hassing H, Montenegro J, Mundt S, Patel S, Card DJ, Hermanowski-Vosatka A, Bergstrom JD, Sparrow CP, Detmers PA, Chao YS. Infectious agents are not necessary for murine atherogenesis. *J Exp Med*. 2000;191:1437–1442.
39. Merat S, Casanada F, Sutphin M, Palinski W, Reaven PD. Western-type diets induce insulin resistance and hyperinsulinemia in LDL receptor-deficient mice but do not increase aortic atherosclerosis compared with normoinsulinemic mice in which similar plasma cholesterol levels are achieved by a fructose-rich diet. *Arterioscler Thromb Vasc Biol*. 1999;19:1223–1230.
40. Teupser D, Persky AD, Breslow JL. Induction of atherosclerosis by low-fat, semisynthetic diets in LDL receptor-deficient C57BL/6J and FVB/NJ mice: comparison of lesions of the aortic root, brachiocephalic artery, and whole aorta (en face measurement). *Arterioscler Thromb Vasc Biol*. 2003;23:1907–1913.
41. Davenport P, Tipping PG. The role of interleukin-4 and interleukin-12 in the progression of atherosclerosis in apolipoprotein E-deficient mice. *Am J Pathol*. 2003;163:1117–1125.
42. Teupser D, Tan M, Persky AD, Breslow JL. Atherosclerosis quantitative trait loci are sex- and lineage-dependent in an intercross of C57BL/6 and FVB/N low-density lipoprotein receptor-/- mice. *Proc Natl Acad Sci U S A*. 2006;103:123–128.
43. Weiss LA, Pan L, Abney M, Ober C. The sex-specific genetic architecture of quantitative traits in humans. *Nat Genet*. 2006;38:218–222.
44. Tamura Y, Adachi H, Osuga J, Ohashi K, Yahagi N, Sekiya M, Okazaki H, Tomita S, Iizuka Y, Shimano H, Nagai R, Kimura S, Tsujimoto M, Ishibashi S. FEEL-1 and FEEL-2 are endocytic receptors for advanced glycation end products. *J Biol Chem*. 2003;278:12613–12617.
45. Kzhyshkowska J, Gratchev A, Brundiers H, Mamidi S, Krusell L, Goerdt S. Phosphatidylinositide 3-kinase activity is required for stabilin-1-mediated endosomal transport of acLDL. *Immunobiology*. 2005;210:161–173.
46. Hansen B, Longati P, Elvevold K, Nedredal GI, Schledzewski K, Olsen R, Falkowski M, Kzhyshkowska J, Carlsson F, Johansson S, Smedsrod B, Goerdt S, McCourt P. Stabilin-1 and stabilin-2 are both directed into the early endocytic pathway in hepatic sinusoidal endothelium via interactions with clathrin/AP-2, independent of ligand binding. *Exp Cell Res*. 2005;303:160–173.
47. Elhage R, Jawien J, Rudling M, Ljunggren HG, Takeda K, Akira S, Bayard F, Hansson GK. Reduced atherosclerosis in interleukin-18 deficient apolipoprotein E-knockout mice. *Cardiovasc Res*. 2003;59:234–240.
48. Aizawa Y, Akita K, Taniai M, Torigoe K, Mori T, Nishida Y, Ushio S, Nukada Y, Tanimoto T, Ikegami H, Ikeda M, Kurimoto M. Cloning and expression of interleukin-18 binding protein. *FEBS Lett*. 1999;445:338–342.
49. Mallat Z, Corbaz A, Scoazec A, Graber P, Alouani S, Esposito B, Humbert Y, Chvatchko Y, Tedgui A. Interleukin-18/interleukin-18 binding protein signaling modulates atherosclerotic lesion development and stability. *Circ Res*. 2001;89:e41–e45.
50. Tiret L, Godefroy T, Lubos E, Nicaud V, Tregouet DA, Barbaux S, Schnabel R, Bickel C, Espinola-Klein C, Poirier O, Perret C, Munzel T, Rupprecht HJ, Lackner K, Cambien F, Blankenberg S. Genetic analysis of the interleukin-18 system highlights the role of the interleukin-18 gene in cardiovascular disease. *Circulation*. 2005;112:643–650.
51. Lutgens E, Faber B, Schapira K, Evelo CT, van Haaften R, Heeneman S, Cleutjens KB, Bijnens AP, Beckers L, Porter JG, Mackay CR, Rennert P, Bailly V, Jarpe M, Dolinski B, Koteliansky V, de Fougerolles T, Daemen MJ. Gene profiling in atherosclerosis reveals a key role for small inducible cytokines: validation using a novel monocyte chemoattractant protein monoclonal antibody. *Circulation*. 2005;111:3443–3452.
52. Weisberg SP, McCann D, Desai M, Rosenbaum M, Leibel RL, Ferrante AW Jr. Obesity is associated with macrophage accumulation in adipose tissue. *J Clin Invest*. 2003;112:1796–1808.
53. George J, Mulkins M, Shaish A, Casey S, Schatzman R, Sigal E, Harats D. Interleukin (IL)-4 deficiency does not influence fatty streak formation in C57BL/6 mice. *Atherosclerosis*. 2000;153:403–411.
54. Lee YW, Kuhn H, Hennig B, Neish AS, Toborek M. IL-4-induced oxidative stress upregulates VCAM-1 gene expression in human endothelial cells. *J Mol Cell Cardiol*. 2001;33:83–94.
55. Walch L, Massade L, Dufilho M, Brunet A, Rendu F. Pro-atherogenic effect of interleukin-4 in endothelial cells: modulation of oxidative stress, nitric oxide and monocyte chemoattractant protein-1 expression. *Atherosclerosis*. 2006;187:285–291.
56. Saleh MC, Wheeler MB, Chan CB. Uncoupling protein-2: evidence for its function as a metabolic regulator. *Diabetologia*. 2002;45:174–187.
57. Ballinger SW. Mitochondrial dysfunction in cardiovascular disease. *Free Radic Biol Med*. 2005;38:1278–1295.
58. Blanc J, Alves-Guerra MC, Esposito B, Rousset S, Gourdy P, Ricquier D, Tedgui A, Miroux B, Mallat Z. Protective role of uncoupling protein 2 in atherosclerosis. *Circulation*. 2003;107:388–390.

Circulation Research
JOURNAL OF THE AMERICAN HEART ASSOCIATION

Identification of Pathways for Atherosclerosis in Mice: Integration of Quantitative Trait Locus Analysis and Global Gene Expression Data

Susanna S. Wang, Eric E. Schadt, Hui Wang, Xuping Wang, Leslie Ingram-Drake, Weibin Shi, Thomas A. Drake and Aldons J. Lusis

Circ Res. 2007;101:e11-e30; originally published online July 19, 2007;
doi: 10.1161/CIRCRESAHA.107.152975
Circulation Research is published by the American Heart Association, 7272 Greenville Avenue, Dallas, TX 75231

Print ISSN: 0009-7330. Online ISSN: 1524-4571